Pure & Appl. Chem., Vol. 60, No. 12, pp. 1841–1864, 1988.
Printed in Great Britain.

Non-equilibrium behavior of small carbohydrate–water systems*

Louise Slade* and Harry Levine

Nabisco Brands Inc., Technology Center, East Hanover, NJ, 07936, USA

Abstract: For pragmatical timescales and conditions (temperature, concentration, pressure), where "real-world" systems are usually far from equilibrium, familiar treatments based on the equilibrium thermodynamics of very dilute solutions fail. Successful treatments require a new approach to emphasize the kinetic description, relate time-temperature-concentration-pressure through underlying mobility transformation, and establish reference conditions of temperature and concentration (characteristic for each solute). Small carbohydrate-water systems provide a unique framework for the investigation of non-equilibrium behavior: definition of conditions for its empirical demonstration, examination of materials properties that allow its description and control, identification of appropriate experimental approaches, and exploration of theoretical interpretations.

INTRODUCTION

Traditional approaches to the study of small carbohydrate-water systems have been divided into four areas (ref. 1). For the single isolated molecule in vacuo, theoretical treatments abound, but experimental approaches are limited; whereas in infinitely dilute solution, various powerful experimental approaches (e.g. spectroscopic) can be applied. These are described in the accompanying review on equilibrium solution properties of polyhydroxy compounds (PHC) by Franks (ref. 2). For a concentrated system (e.g. a solid crystal), in which a single molecule exists in a lattice, a static environment with no time dependence pertains, and X-ray and neutron diffraction provide good experimental data. The fourth area, which for small carbohydrates is the most important for biological and industrial technological applications, is that of very concentrated solutions, where behavior is characterized by great time dependence (refs. 3-9).

One can easily prepare such a concentrated PHC-water system, starting from a dilute solution at equilibrium, by adding solute continuously, until the onset of non-equilibrium thermodynamic effects is observed. However, if one tries to reverse this process, by adding water to a concentrated or dry system in order to return to the original dilute solution state, one observes an extreme hysteresis (refs. 10-12). The time dependence of this behavior is such that it may be impossible, in a practical timeframe, to return to the initial dilute solution from the concentrated system (ref. 13). Similarly, if one wishes to prepare a concentrated solution or melt from a crystalline solid, one can start with either equilibrium crystals (which ordinarily are imperfect, so that the melt would be nucleated on the surface), or a polycrystalline material (where the melt would be nucleated at the interfaces), or a concentrated system (in which the crystal is in equilibrium with the saturated solution), and then apply heat to produce a completely amorphous system. In order to return to the crystalline solid, the system would need to be nucleated. However, the transport properties of such concentrated solutions or melts (of monomeric and polymeric materials, alike) can have a significant adverse effect on their nucleation properties (ref. 35), so that it can prove difficult to nucleate and return to the original crystalline solid. Even if such an amorphous system is pre-seeded, so that homogeneous nucleation is not necessary, one finds, in practical terms, that complete crystallization is never achieved (refs. 14-16). Instead, one obtains a partially crystalline, partially amorphous solid. Thus, whenever one attempts to return a PHC-water system to either the equilibrium crystalline concentrated solid, for which good experimental data are often available, or the infinitely dilute equilibrium solution, to which good experimental methods can be applied, one finds that kinetics and non-equilibrium thermodynamics interfere with the reversibility of such "real-world" systems (refs. 9,17-19).

---

* Invited lecture presented at 8th International Symposium on Solute-Solute-Solvent Interactions (Regensburg, FRG : 9-14 August 1987). Manuscript was not available when other lectures from the Symposium were published (Pure Appl. Chem. Vol. 59, No. 9 (September 1987), pp. 1063-1228)

A NEW APPROACH BASED ON DYNAMICS OF NON-EQUILIBRIUM GLASSY AND RUBERY STATES

A different approach to the four areas of research on small carbohydrate-water systems is needed. One based on a three-dimensional "dynamics map" (i.e. a "functional state" diagram, with axes of temperature, concentration, and time, derived from a more familiar two-dimensional "equilibrium phase" diagram), as shown in Fig. 1, has been suggested (ref. 9). This dynamics map can be expanded to a fourth dimension, conceptually, by incorporating a pressure axis. On such a map, equilibrium conditions can be described in the vapor phase and in the crystalline solid. Such conditions, for the "dry" system, are generally found at relatively high temperatures and very high concentrations of solute. Similarly, for the infinitely dilute system, an equilibrium state can exist, which is usually studied around room temperature. For biological systems, a steady state can be observed at slightly elevated temperatures and higher concentrations. However, the major area of the dynamics map represents a non-equilibrium situation. In order to demarcate this location on the map, one must define a reference state and the timeframe, so that one can make transformations between different relaxation states for a system. Such transformations, as a comprehensive extension of the more familiar time-temperature-transformation (TTT) (ref. 78), will involve temperature, concentration, pressure, and time (or frequency), because each relaxation state actually represents a spectrum of relaxation times, which are themselves time-dependent, and also temperature-, concentration-, and pressure-dependent. "Mobility" will be used as a transcendent principle to connote all of these interdependent concepts embodied in the dynamics map in Fig. 1. Thus, mobility will be the key to all transformations, as well as the basis for defining appropriate reference states. For example, for infinitely dilute solutions, the reference state is 0°K. At this reference state, the kinetic energy goes to zero, but at higher temperatures, there is increasing mobility. In contrast, for technologically practical systems, of higher concentration, the reference state is a glass transition (ref. 20). In this paper, we review the insights that may be achieved by use of the dynamics map, which focuses on the glass transition as the relevant, kinetically-constrained reference state, to construct examples of "mobility transformation maps".

As described in detail elsewhere (ref. 20), the glass transition in amorphous systems is a temperature-, time- (or frequency-), and composition-dependent, material-specific change in physical state, from a "glassy" mechanical solid to a "rubbery" viscous fluid. In terms of thermodynamics, the glass transition is operationally defined as a second order transition and denoted by a) a change in slope of the volume expansion (which is a first-order derivative of the free energy), b) a discontinuity in the thermal expansion coefficient, and c) a discontinuity in the heat capacity (which is a second-order derivative of the free energy).

The glass transition is also operationally defined, based on mechanical properties, in terms of a mechanical relaxation process such as viscosity (η). Figure 2 (ref. 9, adapted from ref. 17) shows that, as the temperature is lowered from that of the low-viscosity liquid state above the crystalline melting temperature (Tm), where familiar exponential Arrhenius kinetics apply, through a temperature range from Tm to the glass transition temperature (Tg), a completely different, very non-Arrhenius, non-exponential, non-linear form of the kinetics becomes operative. Then, at a temperature where mobility becomes limiting, a state transition occurs, typically manifested as a three orders-of-magnitude change in viscosity, modulus, or mechanical relaxation rate (refs. 31,32). A "mechanical" glass transition can be defined by combinations of temperature and deformation frequency for which sufficiently large numbers of mobile units (e.g. small molecules or backbone chain segments of a macromolecule) become immobilized during a time comparable to the experimental period (refs. 33, 34). Exponential Arrhenius kinetics become operative once again in the glassy solid, but the rates of all diffusion-controlled processes are much lower in this high-viscosity solid state than in the liquid state (ref. 9). In fact, the difference in average relaxation times between the two Arrhenius regimes is more than twelve orders of magnitude. In the rubbery range between Tm and Tg, the non-Arrhenius kinetic behavior follows the generic equation (refs. 21,22):

$$\log a_T = \log (\eta/\eta_g) = -[C1(T-T_g)/C2+(T-T_g)] \qquad [1]$$

from the Williams-Landel-Ferry (WLF) free volume interpretation of the glass transition. The WLF eqn. is an empirical equation which describes the effect of increasing temperature on relative relaxation times in glass-forming systems. In the WLF eqn., the coefficient C1 is proportional to the inverse of the free volume of the system at Tg, while C2 is proportional to the ratio of free volume at Tg over the increase in free volume due to thermal expansion above Tg (i.e. ratio of free volume at Tg to the difference between the volumes of the rubbery liquid and glassy solid states, as a function of temperature above Tg) (ref. 20). Note that the reference temperature defined by eqn. [1] is the glass transition temperature. The WLF eqn. is typically used to describe the time-/temperature-dependent behavior of polymers in the rubbery range above Tg, and is based on the assumptions that polymer free volume increases linearly with increasing temperature above Tg and that segmental or mobile unit viscosity, in turn, decreases rapidly with increasing free volume. Mobility is defined in terms of log relaxation rate at a temperature differential above Tg. Thus, the greater the temperature differential, the faster the system is able to move (due to increased free volume and decreased mobile unit viscosity); so the greater is the mobility, and the shorter is the relaxation time. One can also consider this mobility transformation, again in terms of a time/temperature superposition, in the context of measurements of translational diffusion rate (e.g. self-diffusion coefficient), and rotational relaxation rate (e.g. rotational diffusion time), as well as viscosity (ref. 19). For example, the self-diffusion coefficient of water in undercooled solutions of 9-10 w% LiCl changes by five orders of magnitude over a 20° K interval near Tg (ref. 19). This finding is in excellent accord with the behavior predicted by the quantitative form of the WLF eqn., with its "universally"-applicable numerical values of the coefficients C1 = 17.44 and C2 = 51.6, derived from experimental data for many synthetic amorphous polymers (ref. 21). Directly-measured time-temperature-transformation curves have been reported for the crystallization of ice, via homogeneous nucleation, from

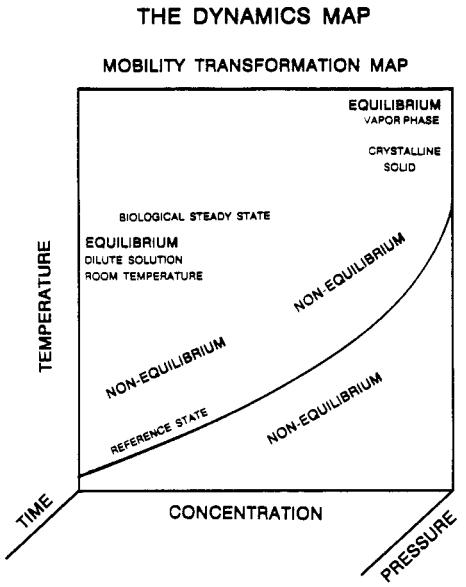

Fig. 1. A four-dimensional "dynamics map", with axes of temperature, concentration, time, and pressure, which can be used to describe mobility transformations.

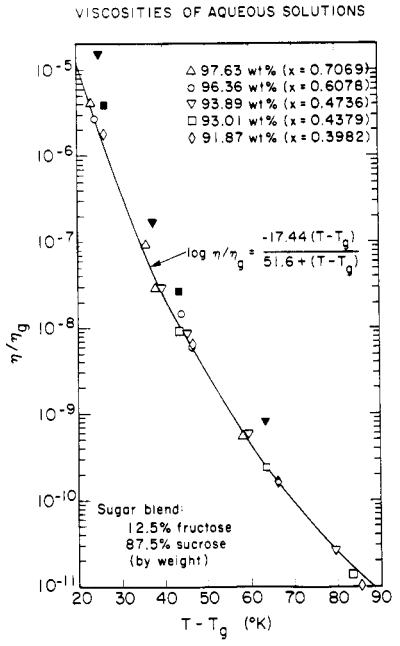

Fig. 3. Temperature dependence of viscosity for aqueous solutions of a 12.5:87.5 (w/w) fructose: sucrose blend, illustrating the fit of the data to the curve of the WLF equation. [Reproduced, with permission, from ref. 22.]

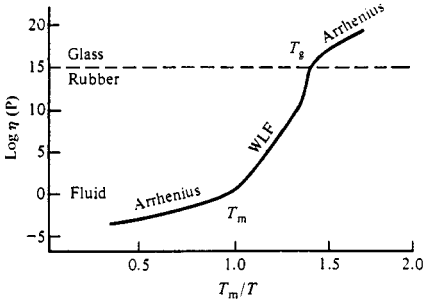

Fig. 2. Viscosity as a function of reduced temperature (Tm/T) for glassy and partially-crystalline polymers. [Reproduced, with permission, from ref. 9.]

the same 9-10 w% LiCl solutions (ref. 78). In the context of the utility of the WLF eqn., the underlying basis of the principle of time/temperature superpositioning is the equivalence between time (or frequency) and temperature as they affect the molecular relaxation processes that influence the viscoelastic behavior of glass-forming small molecule and polymeric materials (refs. 20,54).

The effects of temperature and concentration on the mobility of fluids above Tg can be combined to create a single master curve, which represents the WLF eqn.. The viscosity data shown in Fig. 3 (ref. 22) were obtained for highly concentrated (> 90 w%) aqueous mixtures of fructose and sucrose. These results, like those described above for LiCl solutions, show a five orders-of-magnitude change in the viscosity of concentrated sugar solutions, over a 20°K interval near Tg, which is characteristic of WLF behavior in the rubbery fluid range. These results constituted the first experimental demonstration that concentrated fructose and sucrose solutions obey the WLF eqn. quantitatively as well as synthetic high polymers. Similarly, it had been shown previously that a completely amorphous glucose melt, in the absence of diluent, has the same coefficients in the WLF eqn., and thus also behaves like a typical well-behaved synthetic high polymer (refs. 21,75).

WLF-BEHAVIORAL CHARACTERISTICS OF KINETICALLY METASTABLE POLYMERS

For this paper on small carbohydrate-water systems, we use the word polymer generically to include any homologous series of monomeric and oligomeric PHCs. In that context, we have examined and compared the WLF behavior of kinetically-metastable PHC polymer systems (refs. 6, 9) to the corresponding knowledge base for synthetic high polymers. According to the conventional description, a typical well-behaved synthetic high polymer (e.g. a representational elastomer) would manifest its Tg around 200°K in the completely amorphous state, and its Tm around 300°K in the completely crystalline state (ref. 16), so that the ratio of Tm for the pure crystalline material to Tg for the completely amorphous material is about 1.5 (or Tg/Tm about 0.67) (ref. 23). Such a polymer would also have a macroscopic viscosity of about 10^{12}

Pa s and a free volume fraction of about 2.5% at Tg (ref. 20). For this typical well-behaved polymer, WLF kinetics are considered to be operative in a temperature range about from Tg to 100°K above Tg (ref. 21). It can be seen that this operational definition is related to the typical Tm/Tg ratio of 1.5, since, in such a case, the difference in temperature between Tg and Tm would be about 100°K. Figure 4A illustrates the conventional description of the relaxation behavior of a typical well-behaved polymer (e.g. polyvinyl acetate (refs. 24,75)), which would obey the standard form of the WLF eqn. with the coefficients C1 = 17.44 and C2 = 51.6. As mentioned above, the same coefficients have been observed for amorphous glucose in the absence of diluent (refs. 21,75). In this plot of log a_T vs. ΔT, the relaxation rate progresses from WLF behavior very near Tg to Arrhenius behavior at about 100°K above Tg. Within this temperature range, where technological process control would be expected, relaxation rates for WLF behavior near Tg would change by a factor of 10 for every 3°K change in temperature. In contrast, for Arrhenius behavior with familiar Q10 kinetics above Tm, a factor of 10 change in relaxation rate would require a 33°K change in temperature.

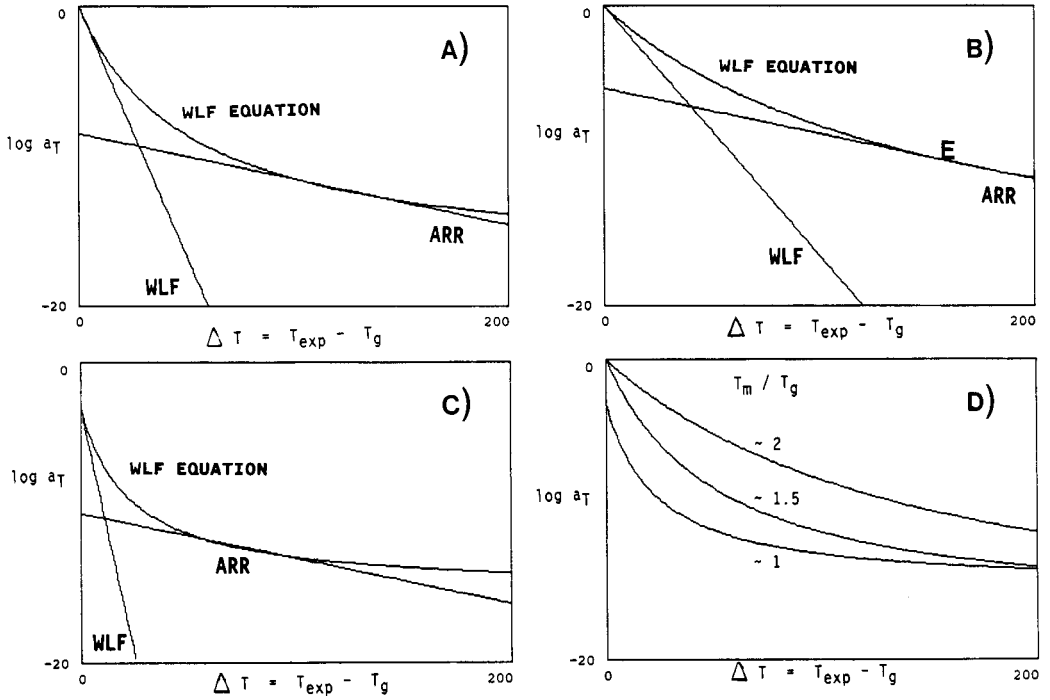

Fig. 4. WLF plots of the time-temperature scaling parameter (WLF shift factor), a_T, as a function of the temperature differential above the reference state, Tg, with the limiting regions of low and high ΔT defined by the WLF and Arrhenius kinetic equations, respectively. The curves of the WLF equation (with coefficients C1 and C2 in eqn. [1] as noted) illustrate the temperature dependence of the relaxation rate behavior for hypothetical polymers with Tm/Tg ratios of: A) 1.5 (C1 = 17.44, C2 = 51.6); B) 2.0 (C1 = 20.4, C2 = 154.8); C) 1.0 (C1 = 12.3, C2 = 23.3); D) 2.0, 1.5, and 1.0.

One can describe another class of amorphous polymers as typical but not well behaved, in the sense that they are readily crystallizable (refs. 16,20,23,25). Highly symmetrical polymers such as poly(vinylidene chloride) and poly(vinyl cyclohexane), which manifest crystalline melting enthalpies of $\backsimeq$ 170 J/g, fit this class. For such polymers, the ratio of Tm/Tg is frequently >> 1.5, so the temperature range between Tg and Tm is >> 100°K. Different WLF coefficients would be required to describe their relaxation profile, as illustrated by the plot in Fig. 4B drawn for C1 = 20.4 and C2 = 154.8. For a representational case of Tg $\backsimeq$ 200°K (with $\eta_g \gtrsim 10^{12}$ Pa s, and free volume fraction $\backsimeq$ 2.5%) and Tm/Tg $\backsimeq$ 2 (Tg/Tm $\backsimeq$ 0.5), Tm would be $\backsimeq$ 400°K. Thus, there would be about a 200°K region in which relaxation rates would change from WLF behavior near Tg (in this case, by a factor of 10 for every 6°K) to Arrhenius behavior near Tm (by a factor of 10 for every 33°K). A notable example of a material with Tm/Tg $\backsimeq$ 2 is water (ref. 17).

A third class of polymers, often characterized by highly unsymmetrical structures, can be described as atypical and poorly behaved, in that Tg is near Tm (refs. 16,23). For such polymers, with Tm/Tg << 1.5 (i.e. $\backsimeq$ 1.25, or Tg/Tm $\backsimeq$ 0.8), a quantitatively different form of the WLF eqn. would be required to describe their relaxation profile. In this case, as illustrated in Fig. 4C, using C1 = 12.3 and C2 = 23.3, the intercept of log a_T was plotted as $\backsimeq$ -3 for ΔT = 0 (i.e. at Tg), in contrast to Figs. 4A and 4B, where log a_T was defined as 0 at Tg. For a representational polymer in this class, Tg $\backsimeq$ 200°K (with $\eta_g << 10^{12}$ Pa s, and free volume fraction >> 2.5%) and Tm $\backsimeq$ 250°K. Thus, the temperature range in which WLF kinetics would be operative is much smaller than usual. Relaxation rates would change from WLF behavior near Tg (in this case, by a factor of 10 for every 1°K) to Arrhenius behavior above Tm (by a factor of 10 for every 33°K) over a region of only about 50°K. The synthetic polymer cited as the classic example of this behavior, which has been attributed to anomalously large free volume at Tg, is bisphenol polycarbonate, with Tm/Tg $\backsimeq$ 1.18 (ref. 23).

Among the simple sugars, fructose and galactose have also been reported (refs. 6,9) apparently to fit this category, as shown in Table 1.

TABLE 1. Mobility transformation data for small carbohydrate dry glasses. The samples are ranked according to increasing values of Tm/Tg.

Sugar or Polyol	Molecular Weight	Tm °K Dry	Tg °K Dry	Tm/Tg
Fructose	180.2	397.0	373.0 (a)	1.06
Maltotriose	504.5	406.5	349.0	1.16
Galactose	180.2	443.0	383.0 (a)	1.16
Maltose	342.3	402.0	316.0	1.27
Mannobiose	342.3	478.0	363.0	1.32
Mannose	180.2	412.5	303.0	1.36
Ribose	150.1	360.0	263.0	1.37
Turanose	342.3	450.0	325.0	1.38
Sorbitol	182.2	384.0	271.0	1.42
Glucose	180.2	431.0	304.0	1.42
Sucrose	342.3	465.0	325.0	1.43
Xylitol	152.1	367.0	254.5	1.44
-1-0-methyl glucoside	194.2	444.5	302.0	1.47 (b)
Cellobiose	342.3	522.0	350.0	1.49
Xylose	150.1	426.0	282.5	1.51
Glycerol	92.1	291.0	180.0	1.62
Glucose:Fructose 1:1	180.2		293.0	

(a) The listed value of Tg for the dry melt is the higher of the two observed values, which governs the mechanical behavior of the water-plasticized glass.
(b) Commercial sample from Staley which was used for mold spore germination experiment of Table 4.

If we compare the three types of behavior exemplified in Figs. 4A-C, in which the Tm/Tg ratio is either the typical value of 1.5, or much greater, or much less, we can examine how the respective relaxation profiles change in the temperature interval between Tm and Tg for representational polymers with a common value of Tg. As illustrated in Fig. 4D, this analysis reveals the critical significance of the Tm/Tg ratio for any given polymer. For a common value of Tg, different values of Tm/Tg for different polymers (such as PHCs) can be used to compare relative mobilities at Tg and at T >> Tg (as demonstrated later with regard to Fig. 11 and Table 4). For different values of Tg, relative mobilities can be compared based on values of the difference, Tm – Tg, rather than the ratio, Tm/Tg, (as illustrated later with regard to Fig. 15). In Fig. 4D, the behavior of log a_T is compared for different values of Tm/Tg (i.e. about 2, 1.5, and the extreme case of 1.0), to determine how mobility varies in the kinetically-constrained regions of this mobility transformation map. At T >> Tg, the overall free volume for different polymers may be similar (ref. 20), yet individual free volume requirements for equivalent mobility may differ significantly, as reflected in the Tm/Tg ratio. The anisotropy in either rotational mobility (which depends primarily upon free volume (ref. 20)) or translational mobility (which depends primarily upon local viscosity, as well as free volume (ref. 20)) may be the key determinant of a particular polymer's relaxation behavior. The glass transition is a cooperative transition (ref. 26) resulting from local cooperative constraints on mobility, and Tg represents a thermomechanical property controlled by the local small molecule or segmental, rather than macroscopic, environment of a polymer. On cooling a viscous fluid of relatively symmetrical mobile units with relatively isotropic mobility, translational motions would be expected to be "locked in" at a higher temperature before rotational motions, because of the slower structural relaxations associated with the larger scale translational diffusion (refs. 27,28). In this case, cooperative constraints of local viscosity and free volume on translational diffusion determine the temperature at which the glass transition is manifested, as a dramatic increase in relaxation times compared to the experimental timeframe. However, in the case of motional anisotropy, molecular asymmetry has a much greater effect on rotational than translational diffusion, so that rotational motions could be "locked in" before translational motions as the temperature is lowered (refs. 29,30). As illuminated by Fig. 4D, a very small ratio of Tm/Tg (i.e. close to 1.0) is accounted for by an anomalously large free volume requirement for rotational diffusion (ref. 23). When the free volume requirement is so large, a glass transition (i.e. vitrification of the rubbery fluid) on cooling can actually occur even when the local viscosity of the system is relatively low. Thus, instead of the typical "firmness" for a glass ($\simeq 10^{12}$ Pa s), such a glass (e.g. of bisphenol polycarbonate, fructose, or galactose) may manifest a $\eta_g << 10^{12}$ Pa s (refs. 4,9,22). In such a glass, the time constant for translational diffusion may be anomalously small, indicative of high translational mobility. In contrast, in the glass of a typical well-behaved polymer, the time constant for translational diffusion would be greater than that for rotational diffusion, so that an increase in local viscosity would be concomitant with a decrease in free volume (ref. 28).

THE MOBILITY TRANSFORMATION MAP

One can begin to build a generic mobility transformation map upon a foundation of established structure/property relationships for typical synthetic amorphous high polymers. For example, the effect of polymer plasticization by non-crystallizing diluents is well known (ref.

37) and nicely illustrated by Tg results for polystyrene solutions with various compatible organic diluents which can be undercooled without crystallizing (ref. 20, Fig. 17-1, p. 488). Characteristically, the Tg of an undiluted polymer is much higher than that of a typical low molecular weight (MW), glass-forming diluent. As the diluent concentration of the solution increases, Tg decreases monotonically, because the average MW of the homogeneous polymer-plasticizer mixture decreases, and its free volume increases.

In contrast, the effect of polymer plasticization by a crystallizing diluent has been illustrated by Tg results for blends of poly(vinyl chloride) (PVC) with a terpolymeric organic plasticizer which is able to crystallize on undercooling (ref. 36). In this interesting case of a polymer and plasticizer with more nearly equal MWs, while the diluent depresses the Tg of the polymer in the typical fashion, the polymer simultaneously depresses the crystallization temperature (Tc) of the plasticizer. Thus, with increasing PVC concentration in the blend, Tc of the plasticizer decreases as Tg of the blend increases. Upon cooling, crystallization of the plasticizer can no longer occur, within a realistic experimental timeframe, in the region (on the state diagram) of temperature and blend composition where the extrapolated crystallization curve intersects the glass curve at a particular point (ref. 36, Fig. 29, p. 892), which can be designated as Tg'. Below a critical diluent concentration (i.e. the composition of the glass at Tg'), crystallization on cooling of the plasticizer, which would be readily-crystallizable if pure, essentially ceases at an incomplete extent, due to the immobility imposed by the vitrification of the glass-forming plasticizer-polymer blend. The analogy between this example of the behavior of a non-aqueous high-polymer system, with its characteristic Tg' and corresponding composition Cg', and the general behavior of aqueous glass-forming systems of small PHCs (discussed below and described with regard to the state diagram in Fig. 5) is important and fundamental to interpreting the non-equilibrium behavior of PHC systems in the context of mobility transformations.

Starting at room temperature with a dilute aqueous solution of a typical small PHC, slow cooling inevitably leads to freezing of ice (i.e. phase separation via crystallization of the diluent). Freezing proceeds with a concomitant change in composition of the non-ice portion of the solution, initially along the path of the equilibrium liquidus and finally along the non-equilibrium segment of the liquidus, to a solute-specific composition of maximum solute concentration. Continued cooling beyond this point produces a glass with a characteristic Tg (denoted by Tg'), solids content (Cg'), and unfrozen water content (Wg') (refs. 3-9,17-19). This maximally freeze-concentrated glass is one particular glass on the continuous glass curve for any specific PHC-water system. In other words, for any solution with an initial water content (W) greater than the solute-specific composition corresponding to Wg', slow cooling causes a change in composition as well as ice formation. In comparison, cooling of the same solution rapidly enough to permit complete vitrification without ice formation, followed by rewarming to a kinetically-metastable condition (i.e. within the map region of $Tg < T < Tg'$ and $W > Wg'$) where ice crystallization can occur, leads to disproportionation and arrival at the same characteristic Tg' and composition Wg' (refs. 3,17,39). Yet another route to the same focal point on the map can be followed by adding diluent to a dry PHC. In this case, Tg decreases to Tg', as the water content increases to Wg'. Any further increase in water content, followed by slow cooling, results in crystallization of the excess plasticizer and, once again, the characteristic Tg' and composition for the non-ice portion. Thus, for diluent concentrations less than Wg', which represents the maximum amount of unfrozen, plasticizing water that can persist in the freeze-concentrated, dynamically -constrained glass at Tg' (ref. 7), a microscopic reversibility is possible. The composition can remain unchanged as the temperature is cycled above and below Tg. Of course, the behavior described above presupposes that the PHC solute does not crystallize (via eutectic crystallization of both solute and solvent) as a consequence of undercooling. If the solute can also crystallize during the experimental timeframe, the possibility of microscopic reversibility can be lost. Instead, the system would exist in a metastable state within the map region between the crystalline melting curve and glass curve for the solute, as well as within the corresponding region for the solvent.

The effect of plasticization of water-compatible polymers by water, a crystallizing diluent, has recently been reviewed elsewhere (refs. 9,45). Tg curves have been reported for various water-plasticized solutes, including PHCs such as sorbitol (ref. 46) and starch (refs. 12, 47-49), proteins such as gelatin (ref. 50), collagen (ref. 51), elastin (ref. 52), and wheat gluten (ref. 53), and synthetic polymers such as PVP (ref. 3) and nylon 6 (ref. 51). The effect of water plasticization is illustrated in Fig. 5, which shows experimental data for the glass curves of the small PHCs, glucose, fructose, and sucrose, and a 40,000 MW poly(vinylpyrrolidone) (PVP-40) (ref. 9). This mobility transformation map for these common sugars and PVP was constructed from measured values of a) Tg of the completely-amorphous, dry solute and b) Tg' and Cg' of the maximally freeze-concentrated glass, coupled with c) the extrapolated, but widely-accepted literature value for Tg of amorphous solid water, $\simeq 140^{\circ}K$ (ref. 17), d) Tm of pure ice, and e) the equilibrium (ref. 38) and non-equilibrium portions of the liquidus curve. Figure 5 reveals that the maximum practical (i.e. spacially homogeneous) dilution of each amorphous solute corresponds to a particular glass in each continuum of glassy compositions. As described above, alternative paths, such as drying by evaporation or freeze-concentration (refs. 5,17,42), lead to the same operationally-invariant composition (Cg'), with its characteristic Tg'. The elevation of Tg, due to increased solute concentration, dramatically affects the shape of the non-equilibrium, very non-ideal portion of the liquidus curve. In other words, the extreme departure from the equilibrium liquidus curve for each of these solutes is related to the shape of the corresponding glass curve. The locus of Tg' on the transformation map depends on both the free volume and local effective viscosity, and therefore on the inverse number-average MW ($\bar{M}n$) and inverse weight-average MW ($\bar{M}w$), respectively (ref. 20), of the dynamically-constrained, kinetically-metastable solution.

Thus, we suggest that the anomalous shape of the extrapolated liquidus curve is a consequence of the system's approach to the immobile, glassy domain, rather than the cause of the

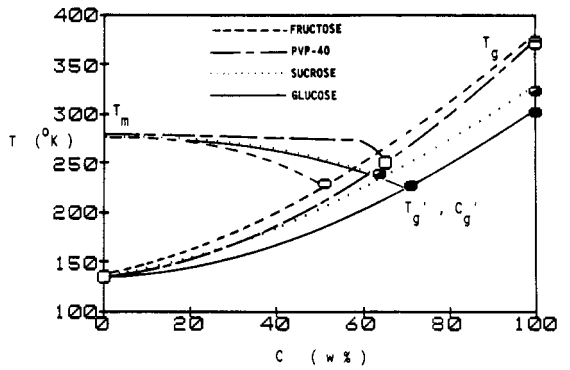

Fig. 5. Solute-water state diagrams of temperature vs. concentration for fructose, glucose, sucrose, and PVP-40, which illustrate the effect of water plasticization on the experimentally-measured glass curves, and the location of the invariant point of intersection of the glass curve and the non-equilibrium portion of the liquidus curve at Tg' and Cg', for each solute.

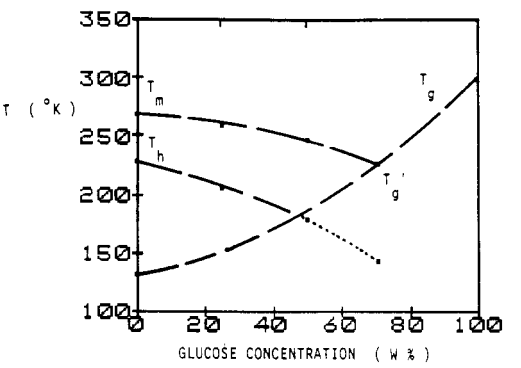

Fig. 6. Glucose-water state diagram, which illustrates the relationship between the locations on this mobility transformation map of the curves for the glass transition temperature, Tg, the melting temperature, Tm, and the homogeneous nucleation temperature, Th.

particular location of the glass at Tg'. The anomalous shape of the liquidus, which has been described elsewhere (ref.19), reflects the non-equilibrium melting behavior of the ice and the improbably low values of apparent relative vapor pressure of the solution that result from the constrained approach to the glassy domain, which represents the limiting range of relaxation rates compared to the timeframe of observation. Equally anomalous values have been observed for the relative vapor pressures of aqueous supra-glassy solutions of PHCs at ambient temperature (refs. 4,9), as described later with regard to Table 4. In both of these situations, the apparent relative vapor pressures are often referred to as water activities, even though they are clearly non-equilibrium values, controlled by, rather than controlling, the long relaxation times of the sytem.

Figure 6 illustrates the effects of a small PHC solute on the non-equilibrium thermodynamic properties of partially-crystalline water, and focuses on glucose as an example of a typical, well-behaved, water-compatible polymer with a Tm/Tg ratio of 1.42. This dynamics map shows the effect of glucose addition on the Tg of water (in terms of measured values of Tg of the spacially-homogeneous aqueous glass), the Tm of phase-separated ice, and the homogeneous nucleation temperatures (Th) of undercooled solutions (ref. 17). Glucose elevates the Tg of water, through Tg', up to the Tg of dry amorphous glucose, by its direct effect on the free volume and local effective viscosity of the resulting sugar-water solution (ref. 20). At concentrations approaching infinite dilution, glucose affects the shape of the liquidus curve by colligative depression of the equilibrium Tm, and also depresses the non-equilibrium Th (ref. 35) of ice. However, at finite glucose concentrations in the range of technological importance, there is a non-colligative, very non-equilibrium effect of the solute on Tm, and a similarly-anomalous effect on Th. The changes in Tm and Th are empirically related by the ratio $\Delta Th/\Delta Tm \cong 2$ (ref. 17). Thus, at practicable concentrations of glucose, effective values of vapor pressure, osmotic pressure, Tm, Th, and crystal growth rate are all INSTANTANEOUS values, determined by the effective relaxation time of the supra-glassy solution. The dotted portion of the Th curve extrapolated below the Tg curve was included in Fig. 6 to allude to the fact that such instantaneous values may persist for centuries (e.g. crystal growth rate of ice in an undercooled PHC-unfrozen water glass (ref. 40)). Indeed, the very enormity of the time-dependence beguiles with the appearance of equilibrium (e.g. kinetics of water ad/absorption via diffusion in amorphous solids, discussed later with regard to Fig. 13 (ref. 13), or water desorption "equilibration" of partially-crystalline, rubbery substrates (ref. 11)).

Figure 7 illustrates the effects of pressure, in the absence of solute, on the same non-equilibrium thermodynamic properties of partially-crystalline water described in Fig. 6, i.e. the Tg of pure amorphous solid water, the Tm of pure crystalline solid ice, and the Th of undercooled liquid water (ref. 17). Increasing pressure elevates the Tg of numerous chemically and thermomechanically diverse polymers by about 20 $\pm$ 5°K per kilobar (100 MPa) (refs. 20,76). The curve of predicted Tg values in Fig. 7 was calculated on the basis of this same behavior for glassy water, which would show conventional volume expansion upon softening. Increasing pressure also depresses the Tm and Th of ice, an effect related to water's anomalous volume decrease upon melting (ref. 17). The changes in Tm and Th produced by increasing pressure are empirically related by the ratio $\Delta Th/\Delta Tm \cong 2$ (ref. 19), curiously analogous to the effect of solute cited above. Thus, Fig. 7 demonstrates that as Tg increases, both Tm and Th decrease anomalously. It should be recalled that a 20°K change in Tg caused by a pressure change of 1 kilobar would be comparable to a five orders-of-magnitude change in mechanical relaxation rates near Tg.

The effects of a small PHC solute can be compared to the effects of pressure on the same non-equilibrium thermodynamic properties of partially-crystalline water, by combining the results in Figs. 6 and 7. As illustrated in Fig. 8, the concentration and pressure scales were

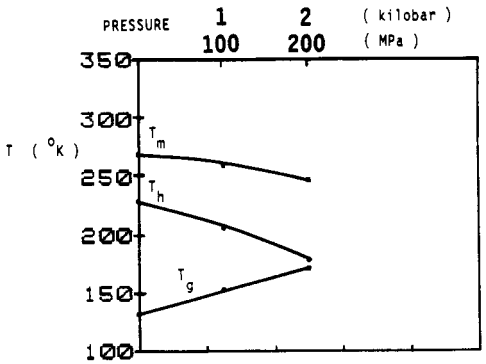

Fig. 7. State diagram of temperature vs. pressure for pure water, which illustrates the effect of increasing pressure on the Tm, Th, and Tg curves.

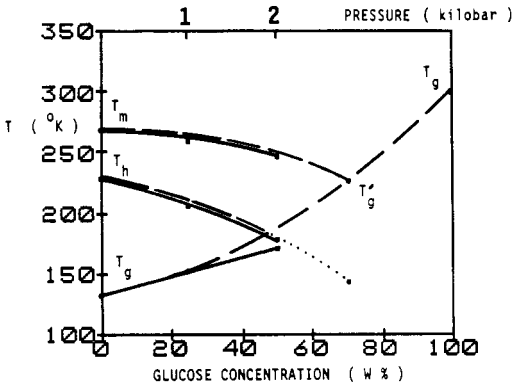

Fig. 8. A superposition of the state diagrams in Figs. 6 and 7, which illustrates the comparison between the effects of added glucose solute and increasing pressure on the non-equilibrium thermodynamic properties of water, in terms of its Tm, Th, and Tg.

overlaid on this mobility transformation map so that we could compare the Tg of glucose -water glasses, the Tm of phase-separated ice in glucose solutions, and the Th of undercooled glucose solutions, all at atmospheric pressure, to the corresponding values of the predicted Tg of amorphous solid water alone, the Tm of pure crystalline ice, and the Th of undercooled liquid water, all up to 2 kilobar. Figure 8 shows that glucose, representing a well-behaved molecular glass former, at concentrations up to $\backsimeq$ 25 w% in the glass, mimics high pressure in its effects on the thermomechanical behavior of water. Both an increase in solute concentration and an increase in pressure result in an elevation of Tg and a concomitant depression of both the non-equilibrium Tm and Th (related by the same ratio $\Delta Th/\Delta Tm \backsimeq 2$). By avoiding the eutectic behavior (i.e. ice I plus ice III) observed at pressures above 2 kilobar for water alone (ref. 19) and instead allowing complete vitrification, higher solution concentrations of glucose ($\gtrsim$ 70 w%) have an even more drastic effect than pressure on the shapes of the non-equilibrium liquidus and Th curves. So, while high pressure alone is not efficient for the prevention of ice formation, glucose solutions at high concentration, or solutions of other even more-ready aqueous glass formers such as LiCl at much lower concentration ($\backsimeq$ 10 w%) (ref. 41), can be completely vitrified by cooling at atmospheric pressure. The additive effects of pressure and small PHC solute would allow complete vitrification at intermediate solution concentrations.

Taken together, the results in Figs. 5-8 summarize the effects of water on the thermomechanical behavior of common sugars and the effects of pressure and common sugars on the non -equilibrium thermodynamics of partially-crystalline water and aqueous solutions. The aqueous glass curves in Fig. 5 can be compared, with emphasis on the striking difference in location on the mobility map of the curves for the two monosaccharides, fructose and glucose, a finding recently reported and discussed (refs. 4,9). This comparison shows that the glass curve for sucrose, at < 50 w% solute, is located closer to that of fructose than glucose, but at > 50 w% solute, sucrose is closer to glucose than fructose. In contrast, PVP-40, at < 50 w% solute, is closer to glucose than fructose, but at > 50 w% solute, PVP-40 is closer to fructose than glucose. The insight derived from these results leads to the new suggestion that different portions of the glass curve must be controlled by different parameters which determine molecular-level mobility, i.e. Tg is controlled by free volume (a function of inverse $\overline{Mn}$) rather than local viscosity at higher values of average MW (i.e. higher solute concentrations in the glass, Cg), but by local viscosity (a function of $\overline{Mw}$) rather than free volume at lower values of average MW (i.e. higher water concentrations in the glass, Wg).

The origin of the empirical ratio $\Delta Th/\Delta Tm \backsimeq 2$ (refs. 17,19) was previously obscured by the expectation that the liquidus curve must be colligatively-controlled while the Th curve is in part diffusion-controlled. The results in Figs. 5-8 illustrate the parallel dynamic control over the non-equilibrium regions of both the liquidus and nucleation curves. Figure 5 also points out that, at solute concentrations > 20 w%, fructose and glucose (of equal MW) solutions have very different Tm, as well as Tg, profiles. So at these PHC concentrations (which are technologically the most important), the Tm curve is certainly not an equilibrium liquidus, but rather a non-equilibrium melting profile, which is affected by the underlying glass behavior. Once again, the explanation for this behavior derives from the WLF kinetics governing the rubbery domain near Tg, where a 20°K temperature interval is equivalent to a range of five orders-of-magnitude in relaxation rates. Hence, within practical timeframes, the immobility imposed by the glassy domain can have an all-or-nothing effect on homogeneous nucleation and crystal growth.

As mentioned earlier, the effect on water of glucose concentrations up to 25 w% mimics the effect of pressure up to 100 MPa, and is nearly equivalent up to 50 w% glucose and 200 MPa pressure. However, while still higher pressure leads to nucleation of ice II or growth of ice III (ref. 17), glucose concentrations > 50 w% lead to continued elevation of Tg and so steadily increasing inhibition of all diffusion-controlled processes, including nucleation and crystal growth of ice. As a consequence, the lower limit of Th, to which pure water

under high pressure can be undercooled without freezing, is ≃ 183°K (ref. 17). In contrast, a glucose solution, of C > Cg' ≃ 70 w%, can be undercooled without limit, and complete vitrification will prevent ice formation in practical timeframes. In fact, Franks has calculated that the linear growth rate of ice, in an undercooled aqueous glass of typical viscosity, η_g at Tg of ≃ 10^{13} Pa s, would be about 10,000 years/cm (ref. 40). Finally, it should be noted that, as a consequence of the differences between the map locations of the glass curves for fructose and glucose, the effect of fructose on the behavior of water is very different from the effect of pressure. Even at concentrations as low as 20 w%, fructose causes a much greater elevation of the Tg of water and, concomitantly, a greater departure from the equilibrium liquidus curve.

EFFECT OF MOLECULAR WEIGHT ON THE MOBILITY TRANSFORMATION MAP

Let us examine the expected effect of MW on the mobility transformation map. For pure synthetic polymers, in the absence of diluent, Tg is known to vary with MW in a characteristic manner. For a homologous series of amorphous linear polymers, Tg increases with increasing MW, due to decreasing free volume contributed by chain ends, up to a plateau limit for the region of "entanglement coupling" in rubber-like viscoelastic random networks (typically at MW = 1,250 - 100,000) (ref. 44), then levels off with further increases in MW (refs. 20,43). The glass at Tg' is not that of the pure, undiluted polymer, and so there is no theoretical basis for assuming that this Tg of the freeze-concentrated glass should depend on MW of the dry polymer. However, if the relative shapes of the polymer-diluent glass curves are similar within a polymer series, increases in MW lead to proportional increases in both Tg and Tg'. Thus, it was recently shown, for two extensive series of PHCs, that the linear relationship between Tg and inverse MW of the solute does apply to the characteristic Tg' of the solute -unfrozen water glass (refs. 3,5,8). For one homologous series of commercial, polydisperse glucose oligomers and high polymers derived from starch, with MWs from 180 for glucose itself to ≃ 60,000 for a 360 DP (degree of polymerization) polymer, Tg' increased with decreasing inverse MW (with a linear correlation coefficient r = -0.98), up to a plateau limit for entanglement at DP ≃ 18 and MW ≃ 3,000 (ref. 3). For a second, non-homologous series of small, monodisperse PHCs with known MWs in the range 62-1,153, including many different sugars, polyhydric alcohols, and glycoside derivatives, Tg' also increased linearly with decreasing inverse MW (r = -0.934), but the entanglement plateau was not reached (refs. 5,8).

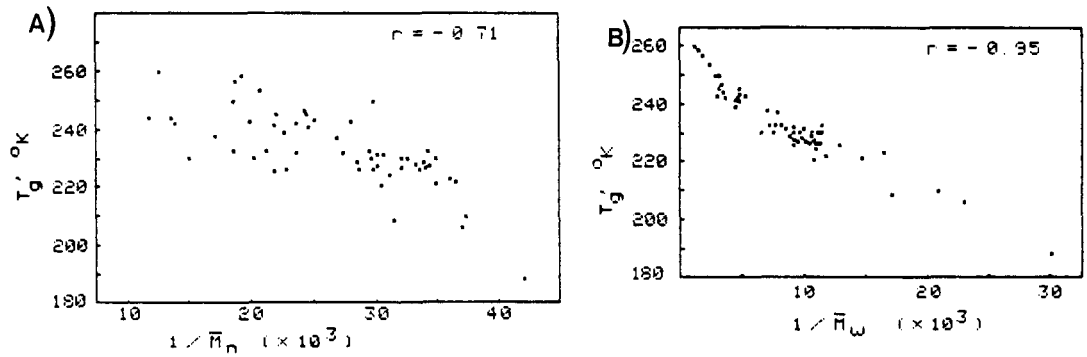

Fig. 9. The variation of Tg' with A) inverse $\bar{M}n$ and B) inverse $\bar{M}w$ calculated from Wg' for the small carbohydrates listed in Table 2.

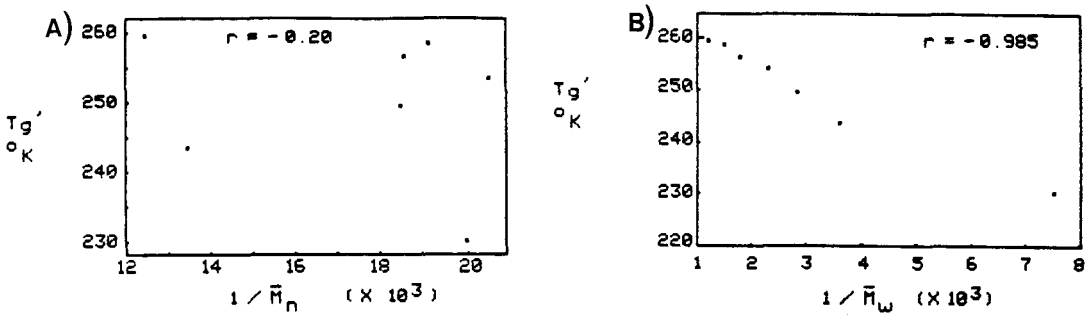

Fig. 10. The variation of Tg' with A) inverse $\bar{M}n$ and B) inverse $\bar{M}w$ calculated from Wg' for the homologous series of malto-oligosaccharides, from glucose through maltoheptaose, listed in Table 2.

For these small PHCs of known MW (see Table 2), the actual $\bar{M}w$ and $\bar{M}n$ of the homogeneous solute-water mixture in the glass at Tg' can be calculated from the corresponding Wg' values, listed in terms of w% water in Table 2. The results were plotted as Tg' vs. $1/\bar{M}n$ and Tg' vs. $1/\bar{M}w$ in Figs. 9A and 9B, respectively. Fig. 9A shows poor linear correlation (r = -0.71) with $\bar{M}n$, which might be expected, because while Tg does vary with free volume of the solution, free volume is most effective as a determinant of Tg when it varies with $1/\bar{M}n$ of the SOLUTE, due to the effect of the number of its molecular chain ends (ref. 20). In contrast,

Fig. 9B shows the much better linear correlation (r = -0.95) of Tg' with $\bar{M}w$ of the aqueous PHC glass, a result which also supports the conclusion that Tg' and Wg' are not independent parameters of the mobility transformation. Within the larger series of non-homologous PHCs in Table 2, the single homologous family of glucose and its linear malto-oligomers up to DP 7 was recently reported to show an excellent linear correlation (r = -0.99) between Tg' and inverse MW of the dry sugar (ref. 9). Again, the relationship between Tg' and the actual $\bar{M}w$ and $\bar{M}n$ of the aqueous glass was examined by comparing plots of Tg' vs. $1/\bar{M}n$ (Fig. 10A) and Tg' vs. $1/\bar{M}w$ (Fig. 10B). These results show even more clearly than those in Fig. 9 that there is no correlation between Tg' and $\bar{M}n$ (r = -0.20), but a very good correlation (r = -0.985) between Tg' and $\bar{M}w$.

TABLE 2. Mobility transformation data for small carbohydrate aqueous glasses. The samples are ranked according to increasing values of $\bar{M}w$.

Polyhydroxy Compound	1 MW	2 Tg' (°K)	3 Wg' (w%)	4 $\bar{M}w$	5 $\bar{M}n$	6 $\bar{M}w/\bar{M}n$	7 Tm/Tg
Ethylene glycol	62.1	188.0	65.5	33.2	23.8	1.39	
Propylene glycol	76.1	205.5	56.1	43.5	27.1	1.61	
1,3-butanediol	90.1	209.5	58.5	47.9	26.9	1.78	
Glycerol	92.1	208.0	45.9	58.1	31.9	1.82	1.62
Erythrose	120.1	223.0	58.2	60.7	27.9	2.17	
Deoxyribose	134.1	221.0	56.9	68.0	28.7	2.37	
Arabinose	150.1	225.5	55.2	77.2	29.7	2.60	
2-O-methyl fructoside	194.2	221.5	61.7	85.5	27.6	3.10	
Deoxyglucose	164.2	229.5	52.6	87.3	31.1	2.80	
Deoxygalactose	164.2	230.0	52.6	87.3	31.1	2.80	
Tagatose	180.2	232.5	57.1	87.6	29.3	2.99	
Arabitol	152.1	226.0	47.1	89.0	33.7	2.64	
1-O-methyl mannoside	194.2	229.5	58.8	90.5	28.7	3.15	
Methyl xyloside	164.2	224.0	50.2	90.7	32.3	2.81	
Ribitol	152.1	226.0	45.1	91.7	34.9	2.63	
Methyl riboside	164.2	220.0	49.0	92.6	33.0	2.81	
3-O-methyl glucoside	194.2	227.5	57.3	93.3	29.4	3.17	
α-1-O-methyl glucoside	194.2	228.5	56.9	93.9	29.6	3.18	
Xylitol	152.1	226.5	42.9	94.6	36.3	2.61	1.44
ß-1-O-methyl glucoside	194.2	226.0	56.3	94.9	29.8	3.18	
Deoxymannose	164.2	230.0	47.4	94.9	33.9	2.80	
1-O-ethyl glucoside	208.2	226.5	57.4	98.9	29.4	3.36	
Fructose	180.2	231.0	49.0	100.8	33.3	3.03	1.06
1-O-ethyl galactoside	208.2	228.0	55.8	102.2	30.2	3.38	
Glucose:Fructose 1:1	180.2	230.5	48.0	102.3	33.7	3.04	
1-O-ethyl mannoside	208.2	229.5	54.8	104.1	30.7	3.39	
2-O-ethyl fructoside	208.2	226.5	53.5	106.5	31.3	3.40	
Ribose	150.1	226.0	32.9	106.7	44.0	2.43	1.37
α-1-O-methyl glucoside (a)	194.2	227.5	49.5	106.9	33.2	3.22	1.47
6-O-methyl galactoside	194.2	227.5	49.5	107.0	33.2	3.22	
2,3,4,6-O-methyl glucoside	236.2	227.5	58.5	108.5	29.2	3.72	
Xylose	150.1	225.0	31.0	109.1	45.8	2.38	1.51
Galactose	180.2	231.5	43.5	109.6	36.6	2.99	1.16
1-O-propyl glucoside	222.2	230.0	55.0	110.0	30.7	3.58	
1-O-methyl galactoside	194.2	228.5	46.2	112.7	35.1	3.21	
1-O-propyl galactoside	222.2	231.0	51.2	117.6	32.6	3.60	
Allose	180.2	231.5	35.9	122.0	42.6	2.87	
1-O-propyl mannoside	222.2	232.5	48.7	122.7	34.0	3.60	
Glucoheptulose	210.2	236.5	43.5	126.6	37.2	3.40	
Sorbose	180.2	232.0	31.0	129.9	47.5	2.74	
Glucose	180.2	230.0	29.1	133.0	49.8	2.67	1.42
Mannose	180.2	232.0	25.9	138.1	54.0	2.56	1.36
Inositol	180.2	237.5	23.1	142.8	58.5	2.44	
Sorbitol	182.2	229.5	18.7	151.5	67.3	2.25	1.42
Mannobiose	342.3	242.5	47.6	187.8	35.7	5.26	1.32
Lactulose	342.3	243.0	41.9	206.5	40.1	5.15	
Isomaltose	342.3	240.5	41.2	208.8	40.7	5.13	
Lactose	342.3	245.0	40.8	209.9	41.0	5.12	
Turanose	342.3	242.0	39.0	215.7	42.6	5.06	1.38
Maltitol	344.3	238.5	37.1	223.2	44.6	5.01	
Sucrose	342.3	241.0	35.9	225.9	45.8	4.93	1.43
Gentiobiose	342.3	241.5	20.6	275.4	72.6	3.80	
Maltose	342.3	243.5	20.0	277.4	74.4	3.73	1.27
Trehalose	342.3	243.5	16.7	288.2	85.5	3.37	
Raffinose	504.5	246.5	41.2	304.2	41.6	7.31	
Stachyose	666.6	249.5	52.8	323.9	33.3	9.74	
Panose	504.5	245.0	37.1	324.0	45.7	7.08	
Isomaltotriose	504.5	242.5	33.3	342.3	50.4	6.79	
Maltotriose	504.5	249.5	31.0	353.5	53.7	6.58	1.16
Maltotetraose	666.6	253.5	35.5	436.5	48.4	9.03	
Maltopentaose	828.9	256.5	32.0	569.6	53.8	10.59	
Maltohexaose	990.9	258.5	33.3	666.6	52.1	12.79	
Maltoheptaose	1153.0	259.5	21.3	911.7	80.0	11.39	

(a) Commercial sample from Staley.

The importance of this finding relates to the concept of the glass transition as an iso-relaxation state. The molecular Tg is not related to macroscopic viscosity, and the origin of the temperature location of the molecular glass transition is not based on an iso-macroscopic viscosity state (ref. 20). Moreover, the location of Tg is not based simply on either an iso-free volume or an iso-local viscosity state alone (ref. 20). For MWs below the entanglement limit (e.g. $\lesssim$ 3,000 for α-1->4 glucan oligomers), the temperature location of the molecular glass transition depends on the instantaneous average relaxation time compared to the experimental timeframe. The operational relaxation time is an instantaneous property, because it depends on the instantaneous values of free volume and local viscosity. Free volume is associated with inverse $\bar{M}n$, rotational relaxation times, high average MWs, and low values of Tm/Tg ratio. Local effective viscosity is associated with $\bar{M}w$, translational relaxation times, low average MWs (e.g. small PHCs), and high values of Tm/Tg ratio. In contrast to the molecular glass transition, for MWs above the entanglement limit, the network Tg does involve macroscopic viscosity.

TABLE 3. The glass transition as an iso-relaxation state. Relaxation parameters are compared on the basis of a common value of Tg (241°K) or particular values of Tg (individual values of Tg').

		Based on Common Tg = 241°K				Based on Particular Tg = Tg'				
Solute	MW	$\bar{M}n$	$\bar{M}w$	$\bar{M}w/\bar{M}n$	Tg-Tg' (°K)	Wg-Wg' (%)	$\bar{M}n'$	$\bar{M}w'$	$\bar{M}w'/\bar{M}n'$	% △
Fructose	180	36	107	3.01	10	-4	33	101	3.03	< 1
PVP-40	40000	46	24407	529	-10	4	51	26006	506	∿4
Sucrose	342	46	226	4.93	0	0	46	226	4.93	
Glucose	180	55	140	2.52	11	-4	50	133	2.67	∿6

To explore the origin of the glass transition in terms of an iso-relaxation state, we compared the glass curves for the four solutes in Fig. 5 on the basis of a common value of Tg, and on the basis of a particular, distinctive Tg, as illustrated in Table 3. For convenience, 241°K (the Tg' of sucrose) was used as a common Tg, equivalent to drawing a horizontal line at Tg = 241°K so that it intersects the glass curves of Fig. 5. The values of Tg', as operationally invariant properties of the individual solutes, were used as a particular Tg. Then for each solute, the values of Wg or Wg' corresponding to the selected values of Tg were used to calculate $\bar{M}n$ and $\bar{M}w$, which govern the relative relaxation behavior. The results in Table 3 show that, for the glasses which would exist at 241°K, those of sucrose and PVP-40 (solutes very different in MW) would have about the same free volume (as indicated by equivalent $\bar{M}n$ values), but very different local effective viscosities (as indicated by the corresponding $\bar{M}w$ values). As a general rule, when two polymeric glasses that have the same $\bar{M}n$ but different $\bar{M}w$ are compared at the same temperature in the absence of diluent, local viscosity increases with increasing polydispersity index, $\bar{M}w/\bar{M}n$ (ref. 20). Importantly, for polymer-plasticizer blends such as PHC-water solutions, both Wg composition of the aqueous glass and MW of the dry solute contribute to the shape of the glass curve, the value of the ratio $\bar{M}w/\bar{M}n$, and the associated relaxation behavior. Thus, the aqueous PVP-40 glass, with a much higher $\bar{M}w/\bar{M}n$ ratio, would have a higher local viscosity than the comparable sucrose glass. The results in Table 3 illustrate that, beyond the general characteristic of $\eta_g \gtrsim 10^{12}$ Pa s at Tg cited for many glass-forming synthetic polymers (refs. 20,26), there is an individuality, so that the glass transition is not rigorously an iso-viscosity state (ref. 20). The absolute viscosity (i.e. "firmness") of the glass at its Tg depends on the nature of the solute, and is thought to vary within the range 10^{11} - 10^{14} Pa s (refs. 3,22,55). However, despite such a range of absolute viscosities at Tg, the respective ranges of relative relaxation rates that would result at T > Tg can all be described by a master curve based on the WLF eqn. with appropriate respective values of the WLF coefficients. The aqueous glass-formers in Table 3 were also compared at their individual Tg' temperatures and characteristic Wg' compositions. These results show, e.g., that while the corresponding $\bar{M}n'$ values for PVP-40 and glucose are similar, indicative of similar free volumes, their $\bar{M}w'$ values are very different. Again, this indicates that the aqueous PVP-40 glass at its Tg' has a much higher local viscosity, and so much longer relaxation times, than the aqueous glucose glass at its Tg'. This comparison sheds light on the underlying mechanism for the greater microbiological stability provided by polymers and proteins than by small PHCs in concentrated solutions with equivalent relative vapor pressures, which has been observed empirically, and ascribed to a hypothetical ability of polymers to "bind" water more tightly (so-called "polymer water") than can small PHCs (so-called "solute water") (ref. 72). The actual mechanism plays an important role in the microbiological experiment discussed later with regard to Table 4. Overall, the results in Table 3 demonstrate that the ratio of $\bar{M}w/\bar{M}n$ provides a better prediction of the shape of the glass curve as an iso-state, which requires a description of both the temperature and the moisture content at which relaxation times become limiting, than does MW or $\bar{M}n$ or $\bar{M}w$ alone.

Figure 11 (adapted from ref. 20) reveals the critical importance of local effective viscosity EVEN AT 100°K ABOVE Tg, and discloses the relationship between this local viscosity, the corresponding translational relaxation time, and polymer Tm/Tg ratio. The figure presents a ranking of values of log [translational friction coefficient] measured at T = Tg + 100°K, for a variety of synthetic polymers. The frictional coefficient was measured in two ways

with equivalent results, as segmental mobility of the polymer backbone and as small molecule diffusion of a reporter (probe) molecule at sufficiently low concentration that there is no measurable depression of Tg due to plasticization. Thus, the translational relaxation time, as reflected by the frictional coefficient or the translational diffusion coefficient, is related to the local effective viscosity surrounding polymer chain segments, rather than to an inherent structural/mechanical feature of the chain itself (ref. 20). Decreasing translational relaxation time correlates with decreasing frictional coefficient, increasing diffusion coefficient, and decreasing local effective viscosity.

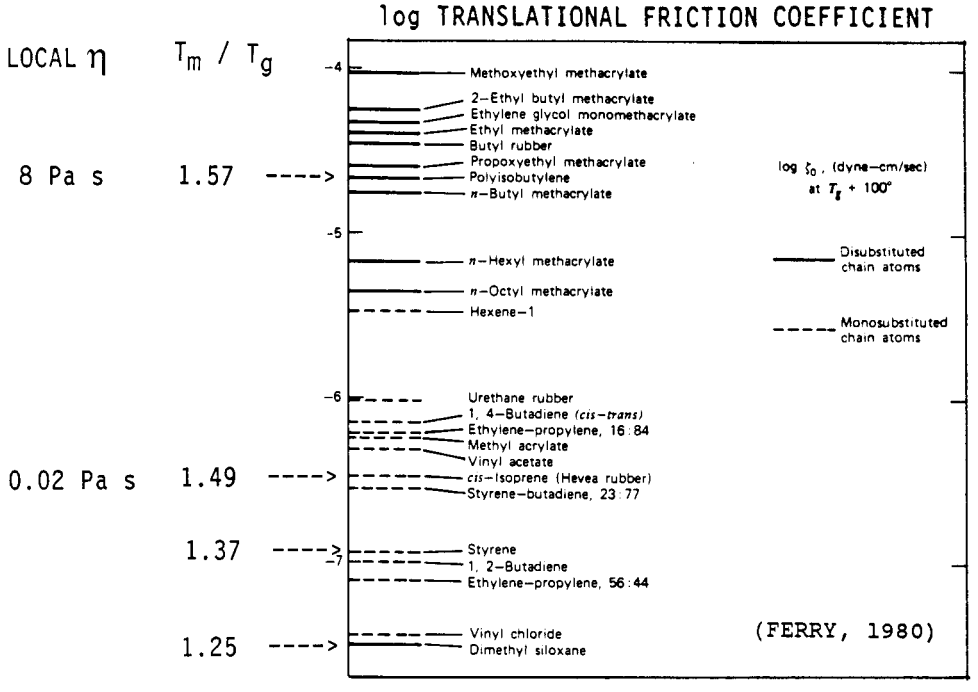

Fig. 11. A ranking of synthetic polymers by their values of log (translational friction coefficient), measured at T = Tg + 100°K, and corresponding values of local viscosity at the same temperature, and Tm/Tg ratio. [The list of ranked polymers reproduced, with permission, from ref. 20.]

It is generally thought that one can best compare and control the behavior of amorphous materials at temperatures at or near their Tg, and that in order to "freeze" events in time and thus magnify the behavioral differences between materials, one must do experiments at T < Tg, where relaxation rates are extremely slow. However, Fig. 11 illustrates that when polymers are studied even 100°K above their individual Tg values, there are orders-of-magnitude differences in the self-diffusion rate of the backbone chain segments or the diffusion rate of small molecules which are similar to the monomer. For example, for poly(isobutylene) and Hevea rubber, at 100°K above their almost identical Tg, there is about a 100-fold difference in the translational diffusion rate of a small reporter molecule, with the Hevea rubber showing the lower local viscosity and lower frictional coefficient and allowing the faster diffusion rate. In the case of poly(dimethyl siloxane), whose low ranking on the list in Fig. 11 has been considered quite anomalous (ref. 20), there had been no previous explanation for why its frictional coefficient and local viscosity, 100°K above Tg, are so low compared, for example, to those of poly(isobutylene). However, addition of the Tm/Tg ratios calculated from reported data for Tm and Tg of these polymers (ref. 20) to Fig. 11 reveals a progressive decrease in this parameter with decreasing local viscosity and frictional coefficient, which in turn reflects an increase in mobility and translational diffusion rate, and a decrease in relaxation time. We suggest that the underlying basis for these behavioral correlations is that the least viscous, and thus most mobile materials, even 100°K above Tg, are those which have the lowest values of Tm/Tg ratio, while the most viscous, least mobile materials are those with the highest Tm/Tg ratios. This correlation in turn supports the conclusion reached earlier, from the analysis of Fig. 4D, that for a common value of Tg (e.g. for the elastomers poly(isobutylene) and Hevea rubber), different values of Tm/Tg ratio for different polymers can be used to compare relative mobilities both at Tg and at T >> Tg. This conclusion is also supported by the results of a revealing biological experiment, analyzed as a mechanical relaxation process, described later with regard to Table 4. It is critical to note that a small difference in the values of Tm/Tg is manifested as a dramatic difference in local viscosity and translational diffusion. In the example described above, the values of Tm/Tg for Hevea rubber and poly(isobutylene) are 1.43 and 1.57, respectively, and the local viscosities at 100°K above Tg differ by nearly two orders of magnitude.

The importance of this correlation between local effective viscosity and Tm/Tg ratio relates to the apparently pivotal influence of these two parameters on the mobility of SUPRA-GLASSY LIQUIDS, such as molten polymers, even well above Tg. This finding can now be coupled with the earlier explanation of how the relationship between η_g, Tm/Tg ratio, and mobility can be

used to characterize the non-equilibrium behavior in the glassy solid state at Tg and in the rubbery fluid state above Tg, and also the size of the temperature domain corresponding to the WLF region. It was mentioned with regard to Fig. 4C that for an atypical, poorly-behaved polymer with Tm/Tg = 1.25, the rubbery region of WLF behavior might only extend about 50°K above Tg. Thus, some of the polymers listed in Fig. 11 (especially, e.g., poly (dimethyl siloxane)), at 100°K above Tg, probably exist as low-viscosity liquids well above their rubbery domain. Yet, the influence of local effective viscosity and Tm/Tg ratio still carries over to their supra-glassy, non-equilibrium behavior. This point is crucial in countering the argument (ref. 11) that sorption hysteresis observed in molten polymers well above their Tg (e.g. concentrated molten synthetic polymer-organic solvent solutions (ref. 56)) cannot be simply explained by linking this behavior to non-equilibrium effects imposed by the properties of the glassy solid state. Analogous hysteresis between water vapor ad/absorption and liquid water desorption in native starch has been reported to result from desorption which remains non-equilibrated even after two years, vs. adsorption which achieves and remains in "well-defined equilibrium" states over the same period (ref. 11). We suggest an alternative explanation for the observed hysteresis, whereby both limbs of the isotherm reflect the persistence of non-equilibrium states. The desorption limb represents the behavior of supra-glassy, partially-crystalline starch drying slowly and irreversibly to a partially-crystalline glassy state (refs. 57,58) different from the original native state. In contrast, the ad/absorption limb represents the behavior of partially-crystalline glassy native starch undergoing an extremely slow, water-plasticized relaxation process (ref. 59), which remains VERY FAR from equilibrium even after two years, to a supra-glassy, partially-crystalline state, i.e. a "pseudo steady state" easily mistaken for equilibrium. This same "pseudo steady state" behavior has been observed for the sorption of water vapor by cod, as described later with regard to Fig. 13 (ref. 13).

It is worth noting that the low values of local viscosity at T = Tg + 100°K shown in Fig. 11 compare to a macroscopic viscosity of about 10^9 Pa s for an entanglement network, and even higher viscosities if the network is crosslinked (ref. 20). This last point and the above discussion of the implications of Fig. 11 underline the importance of research on small PHC-water systems. Synthetic high polymers suffer from the handicaps of unknown, polydisperse MW and MW distribution, and MWs often above their entanglement limit, in which case local effective viscosity is not equivalent to macroscopic viscosity. In contrast, small PHCs, with known, monodisperse values of MW, all below the entanglement limit, so that local effective viscosity is equivalent to macroscopic viscosity, offer a great variety and selection of glass-forming materials for the study of non-equilibrium behavior.

MOBILITY TRANSFORMATION DATA FOR SMALL CARBOHYDRATES

Experimental mobility transformation data for several sugars and polyols are compiled in Table 1. For these pure PHCs of known MW, analyzed in the absence of water, Tm and Tg were measured by differential scanning calorimetry (DSC) (ref. 6). The samples are ranked in Table 1 according to increasing values of Tm/Tg ratio. Of these common sugars and polyols, fructose shows the most extremely anomalous Tm/Tg ratio of 1.06 (refs. 4,6,9). This value is much lower even than the lowest Tm/Tg ratio reported for a synthetic high polymer, i.e. 1.18 for bisphenol polycarbonate (ref. 23). We reported previously that fructose's Tm/Tg ratio of 1.06 derives from the observation of TWO widely-separated glass transition temperatures in a quench-cooled, completely amorphous melt of pure crystalline ß-D-fructose (ref. 9). The lower Tg appears at a lower temperature than the single values of Tg of other common monosaccharides of the same MW, such as glucose and mannose. However, the much higher Tg is readily detectable at 373°K, a temperature only 24°K below the measured Tm of ß-D-fructose. Another monosaccharide, galactose, shows analogous anomalous behavior, with a lower Tg similar to that of glucose and mannose, but a second, much higher Tg similar to the higher Tg of fructose (ref. 6). The observed change in heat capacity at the higher Tg of fructose is smaller in magnitude than at the lower Tg, which may reflect either a smaller actual difference in heat capacity of the fructose population which vitrifies at the higher Tg than of the second, structurally different fructose population which vitrifies at the lower Tg, or that the population of fructose molecules which vitrifies at the higher Tg of the conformationally heterogeneous melt is smaller, while the second population which vitrifies at the lower Tg is larger. However, for reasons explained later, which are based on our interpretation of experimental results (e.g. in Table 4) involving several aspects of the anomalous behavior of fructose in non-equilibrium aqueous systems and processes, we have hypothesized that the higher Tg of fructose (and of galactose as well) is the critical one that defines the Tm/Tg ratio and controls the consequent mobility in its glassy and supra-glassy states (refs. 4,6,9).

With regard to the unusual phenomenon of two values of Tg exhibited by quenched melts of fructose and galactose, Franks (ref. 60) has observed qualitatively-similar anomalous behavior for the same two monosaccharides, and their contrast to well-behaved glucose. Franks has also confirmed our finding that, in a two-component glass with another small sugar (in his case, sucrose), the higher Tg of fructose is no longer detectable, as shown for a 1:1 (w/w) glucose:fructose glass in Table 1, and earlier results for sucrose:fructose mixtures (ref. 22). This change in the thermal behavior of fructose, to become more like glucose in the 1:1 mixture in the absence of diluent, is also manifested in the relative microbiological stability of concentrated solutions of glucose, fructose, and the 1:1 mixture, as will be discussed with regard to Table 4. Among a number of different cases of multiple values of Tg observed in amorphous and partially crystalline systems (refs. 7,45), fructose may represent the interesting situation where two conformationally different populations of the same chemical species manifest different free volume and local viscosity requirements for mobility. Such a situation would arise if one of the conformational populations in a heterogeneous melt exhibited anisotropic rotational and translational mobilities, while the second population exhibited isotropic motion. For motional anisotropy, the free volume requirements for

rotational mobility become much more stringent than those for translation (refs. 29,30), and rotational relaxation would become limiting at a higher temperature than translational relaxation, as described with regard to Fig. 4D for polymers with anomalously low values of Tm/Tg. For isotropic motion, the larger scale, slower translational relaxations become limiting at a higher temperature than rotational relaxations (refs. 28, 29), as described with regard to Fig. 4D for polymers with typical and high values of Tm/Tg. For both anisotropic and isotropic motion, the temperature at which translational relaxations become limiting would be nearly the same. Thus, relaxation times for a conformational population with anisotropic motion would become limiting at a higher temperature, manifested as a higher Tg, than relaxation times for a second population with isotropic motion, manifested as a lower Tg. A documented case, which might provide an explanation for the appearance of two conformationally different populations in a heterogeneous melt from a single crystalline conformation of a single chemical species, involves xylose, which has been shown to undergo rapid anomerization during melting (ref. 61). During the time between heating α-D-xylose to a temperature only slightly above Tm, to avoid decomposition, and quench-cooling the resulting melt to a glass in a conventional DSC experiment, a mixed population of anomers is able to form in the melt and be captured in the glass. Thus, the initial crystal contains only the alpha anomer, while the final glass contains an anomeric mixture of α- and β-xylose, and the particular conformer distribution in the glass depends on the experimental variables of temperature, pressure, and concentration. The fact that only a single value of Tg is observed for the xylose melt, which is known to be conformationally heterogeneous, indicates either that all of the conformers are chemically and mechanically compatible so that a single glass vitrifies, or that all of the glasses that vitrify have the same free volume and local viscosity requirements for mobility and so the same value of Tg. If other small PHCs, such as fructose and galactose, behave like xylose with respect to anomerization during the melting process, then depending on the specific Tm, the time the melt is held above Tm, and the quenching rate, they may also be capable of forming heterogeneous melts with conformationally different populations. Then the fact that two values of Tg are observed would indicate that the two populations are not chemically and mechanically compatible and that they exhibit different free volume and local viscosity requirements for mobility. Franks (ref. 60) made another observation about the higher Tg of fructose that could support such speculation about the possibility of anomerization in a fructose melt. He noted that, after repeated heating and recooling of the initial fructose melt, the magnitude of the observed change in heat capacity at the higher Tg diminished and ultimately became undetectable, leaving only the lower Tg (representing the glass of the more stable anomer?). This observation of changes in the sizes of the two populations upon repeated heating suggests that the difference in magnitude of the observed heat capacity for the two glasses after the initial fructose melt was due to different sizes of the two populations rather than different actual changes in heat capacities. Because fructose is such a technologically important sugar, its glass-forming behavior and the ramifications thereof are a subject worthy and in need of further study.

The results for Tm/Tg ratio in Table 1 show that fructose has the lowest value, based on selection of the higher Tg value as the one of thermomechanical importance, while galactose (along with maltotriose) has the next-lowest. Thus, this fructose glass would be expected to have the highest requirement for free volume in the glass at Tg, and conversely the lowest local effective viscosity ($\lesssim 10^{11}$ Pa s). At the other end of the scale, glycerol, with the highest Tm/Tg ratio, would have the lowest requirement for free volume, but the highest local viscosity ($\cong 10^{14}$ Pa s) in its glass at Tg. Consequently, at their respective values of Tg, a glycerol glass would be predicted to be significantly firmer than a fructose glass.

Experimental mobility transformation data for an extensive list of small carbohydrates, including many sugars, polyols, and glycoside derivatives, are compiled in Table 2 (adapted from ref. 6). These PHCs, of known monodisperse MW (Table 2, col. 1), were analyzed as 20 w% aqueous solutions by low-temperature DSC (refs. 3,5). For each PHC, Table 2 lists the measured Tg' value (col. 2) for the maximally freeze-concentrated glass, which represents the reference state for the analysis that follows. This Table also includes the corresponding Wg' value (w% unfrozen water, col. 3), calculated $\bar{M}w$ (col. 4) and $\bar{M}n$ (col. 5) for the solute -water mixture in the glass at Tg', the corresponding $\bar{M}w/\bar{M}n$ ratio (col. 6), and the Tm/Tg ratios (col. 7) of some of the dry PHCs, from Table 1. The samples are ranked in Table 2 according to increasing values of $\bar{M}w$. In the interest of saving space, two other versions of this Table, with the samples ranked by increasing $\bar{M}n$ or increasing $\bar{M}w/\bar{M}n$ ratio, cannot be shown but will be alluded to, and so are left to the reader to construct.

If Table 2 had been ranked according to solute MW, all of the hexose monosaccharides would have appeared together. But when such common sugars as fructose and glucose are ranked, not according to solute MW, but rather based on the Tg'-Wg' reference state, they are widely separated on the list. The ranking according to increasing $\bar{M}n$ reflects decreasing requirement of free volume for mobility near Tg' for PHCs with the same value of Tg'. Thus, the free volume required for limiting mobility of fructose and captured in the fructose glass ($\bar{M}n$ = 33.3) is much greater than that for glucose ($\bar{M}n$ = 49.8). We conclude that the composition and physicochemical properties of this glass at Tg', which represents the crucial reference condition for technological applications involving any of the common functional properties of a small carbohydrate, cannot be predicted based on the MW of the dry solute. The ranking according to increasing $\bar{M}w$ in Table 2 reflects increasing local effective viscosity in the glass at Tg', for PHCs with the same values of Tg' and $\bar{M}n$. Careful examination of the order of the PHCs in this Table, compared to the different orders resulting from rankings by $\bar{M}n$ and $\bar{M}w/\bar{M}n$, has revealed that the order changes dramatically, depending on whether these small carbohydrates are ranked according to free volume, local effective viscosity, or the ratio of local viscosity/free volume. Significantly, while ethylene glycol appears at the top of all three listings, trehalose appears at the bottom of the listing by $\bar{M}n$ (85.5), reflecting lowest free volume requirement for mobility near Tg' compared to the other disaccharides in the list, while maltoheptaose appears at the bottom of Table 2 ($\bar{M}w$ = 911.7), reflecting very high local viscosity of the glass at Tg', but next to last (preceding malto-

hexaose) in the order of increasing $\bar{M}w/\bar{M}n$ ratio (11.39). So again, we conclude that one cannot predict, based on MW of the dry solute, even for the series of glucose oligomers from the dimer to the heptamer, where such small carbohydrates will rank in terms of the free volume and local viscosity requirements for mobility near the glass at Tg'-Wg'.

In addition to the earlier description of the double-Tg behavior observed for dry fructose and galactose, and the anomerization of xylose, a few more remarks are in order about the unusual phenomenon of multiple values of Tg in glass-forming systems, since this is a subject of increasing current interest (refs. 3-9,33,45,62-65). For systems of compatible glass-formers (including, e.g., aqueous solutions of many of the small PHCs in Table 2), in the absence of devitrification, the solid glass would have identical spatial homogeneity as the corresponding liquid solution, and so a single Tg. In contrast to this familiar case of a quench-cooled, homogeneous glass, there are trivial cases in which more than one Tg may be seen. For instance, due to incomplete phase separation in an incompletely-frozen aqueous solution (refs. 33,63-65), two different dynamically-constrained glasses may co-exist: one, a "bulk" glass, with the same spatial homogeneity as the original dilute solution and a corresponding Tg; and the other, surrounding the ice crystals, the freeze-concentrated glass with a Tg which is Tg' (refs. 3-9). The observation of such a Tg + Tg' doublet depends on sample moisture content, cooling-heating history, and pressure history, and represents an example of the difficulty that can be encountered in deconvoluting the non-equilibrium effects of sample history, and the potential for misinterpretation that can arise when experiments on small PHCs are not designed from a knowledge of the operative reference state (refs. 63-65). Another trivial case involves simple molecular incompatibility in a two-component system, where, due to a lack of spatial homogeneity on a dimensional scale $\gtrsim$ 100 Å (ref. 26), two separate glasses with different values of Tg may co-exist. A non-trivial case of multiple values of Tg can result from a pressure-induced or -facilitated liquid-liquid separation, leading to spatial inhomogeneity in aqueous solutions of, e.g., lithium chloride and tetraalkylammonium halides (ref. 62). Another non-trivial case can result from the formation of specific stoichiometric complexes in aqueous solutions of, e.g., glycerol, DMSO, and lithium chloride (ref. 41), where each complex would exhibit its own discrete Tm (or eutectic melting temperature) and Tg'.

EXPERIMENTAL APPROACH TO DISTINGUISHING EFFECTS OF TRANSLATIONAL AND ROTATIONAL MOBILITY ON MECHANICAL RELAXATION PROCESSES

As emphasized above, small PHCs and their aqueous solutions offer a unique framework for the investigation of non-equilibrium behavior under conditions of importance to technological applications. The small PHCs are monodisperse with known MW below the entanglement limit. They provide several homologous or nearly homologous series of oligomers. They exhibit an astonishing diversity of thermal and thermomechanical properties which can be studied within particular sub-groups: PHCs with the same MW, PHCs with different MW in a homologous series, single PHC with different conformations. Use of the dynamics map as a new conceptual approach to the study of non-equilbrium thermomechanical behavior facilitates the selection of experimental conditions to allow each PHC to be examined at an equivalent distance of moisture and temperature from its respective reference glass curve. For most effective use of the dynamics map as a mobility transformation map to elucidate the underlying basis of the differences in behavior of PHCs, it is necessary to identify appropriate experimental approaches that are capable of separating the effects of translational and rotational mobility on different mechanical relaxation properties. Since local effective viscosity is related to relaxations which are controlled by translational diffusion, it reflects the mobility of the molecular-level environment. Thus, the same relaxation rates and temperature dependence would be expected for results of, e.g., small molecule diffusion, polymer frictional coefficient, and pulsed field gradient-spin echo NMR spectroscopy of PHC-water systems (refs. 66-70).

In general, mechanical relaxations depend on both translational and rotational mobility. For a typical, well-behaved polymer, an increase in free volume would be expected to go hand-in-hand with a decrease in local viscosity. However, when either the rotational or translational relaxation time is the limiting aspect for a particular small PHC-water glass-forming system, the ranking of solutes, i.e. either by $\bar{M}n$ or $\bar{M}w$, would be expected to depend on the underlying mechanism of the specific mechanical relaxation.

Experimental mechanical relaxation processes can be categorized in terms of their control by rotational or translational mobility. For example, homogeneous nucleation depends on both translation and rotation, but can be completely controlled and limited by the rotational mobility (refs. 15,17,35,71). The response to microwaves, in a microwave dielectric dispersion experiment (refs. 66-68,70), is another rotational response. In contrast, the apparent, non-equilibrium relative vapor pressure (RVP) (i.e. the so-called "water activity" or Aw value for biological and food systems) depends on translational mobility (refs. 4,9). Other mechanical relaxation processes controlled by translational mobility include, e.g., starch gelatinization (refs. 47,57,58), mold spore germination (refs. 4,9), and crystal growth (refs. 9,15). A conceptual experimental approach to the study of these various relaxation processes, as they pertain to the non-equilibrium behavior of small PHC-water systems, will be illustrated in the remainder of this paper.

The selection of a molecule to be used as a reporter to probe the local environment is a critical element of experiments to study mechanical relaxation processes. A very low concentration of reporter molecule (e.g. a dye) is required for translational and rotational diffusion experiments, in order to avoid concentration gradients and perturbation of the local relaxation due to plasticization by the reporter (ref. 77). Water itself is NOT a good candidate for the role of reporter molecule to study the mobility of aqueous glasses, because water would then be both a functional part of the sample matrix and a reporter in many ex-

periments. For example, in an NMR investigation of the mobility of water in an amorphous polymer, the water concentration cannot be changed without significantly changing the system itself, because of the effect of water as a plasticizer (ref. 45). Thus, a third molecule would be needed to act as the reporter. Later, we describe how high-polymeric starch can be used to fill this key role. In this context of a discriminating experimental approach, it is worth reiterating that small PHC aqueous glasses are uniquely excellent model systems for the study of non-equilibrium relaxation processes. For solute MWs below the entanglement MW of ≅ 3000 (glucose DP ≲ 18), such non-entangling polymers allow the study of the contributions of free volume and local effective viscosity (as the measured viscosity), without the ambiguity introduced by convolution with the bulk entanglement network viscosity, which would be essentially the same for all polymers (ref. 20). Glass compositions can be measured quantitatively in terms of $\overline{Mn}$ and $\overline{Mw}$. Moreover, in contrast to aqueous glasses of ionic salts, complicating effects due to specific ion hydration and concentration-dependent pK can be avoided.

Homogenous nucleation

On a timescale of technological significance, crystallization can only occur within the kinetically-metastable region of the mobility map between Tm and Tg of the polymer (i.e. the WLF rubbery domain) (refs. 9,15). In the process of crystallization for a polymer which is completely amorphous and unseeded, homogeneous nucleation in an undercooled melt is the first mechanistic stage, which must precede crystal growth. The necessary extent of undercooling in °K from Tm to Th, the homogeneous nucleation temperature, is a universal property of crystallizable materials. Just as Tg is related to Tm by the ratio Tm/Tg ≅ 1.5, with a range of 1 to 2, for essentially all molecular glass formers, including small molecules and high polymers, Th is related to Tm by the ratio Tm/Th ≅ 1.25, with a narrow range of 1.17 to 1.28 for essentially all crystallizable substances, including metals, salts, small organic molecules, and high polymers (refs. 15,71). For the representational typical elastomer (Fig. 4A) with Tg = 200°K and Tm = 300°K, the calculated Th value would be 240°K.

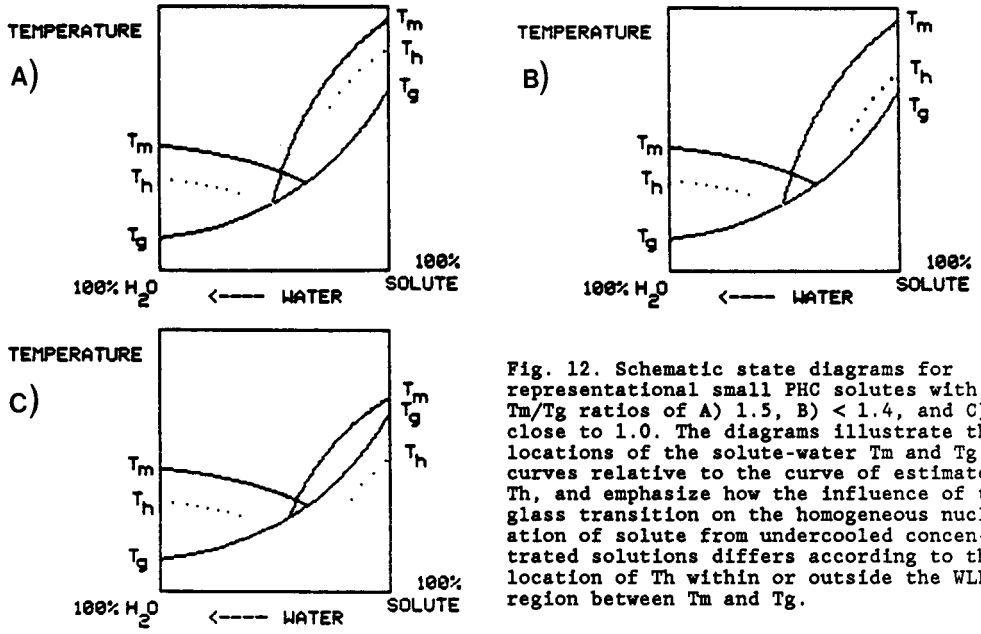

Fig. 12. Schematic state diagrams for representational small PHC solutes with Tm/Tg ratios of A) 1.5, B) < 1.4, and C) close to 1.0. The diagrams illustrate the locations of the solute-water Tm and Tg curves relative to the curve of estimated Th, and emphasize how the influence of the glass transition on the homogeneous nucleation of solute from undercooled concentrated solutions differs according to the location of Th within or outside the WLF region between Tm and Tg.

The relationship between Th, Tm, and Tg, for representational small PHCs in water is illustrated in Fig. 12, which shows schematic state diagrams for three different situations that can govern homogeneous nucleation. The situations result from different values of the ratio Tm/Tg, which reflects the magnitude of the metastable WLF region in which crystallization can occur. In each case, Th was located according to the typical ratio of Tm to Th. These stylized state diagrams highlight the different ways in which Th and Tg can be related, depending on the Tm/Tg ratio for a particular PHC solute, and thus reveal how the relationship between Th and Tg determines and allows prediction of the stability against recrystallization of concentrated or supersaturated aqueous solutions of specific PHCs (ref. 9). In the first case (Fig. 12A), for a PHC with a typical, higher Tm/Tg ratio of ≅ 1.5, homogeneous nucleation of the solute would be very efficient, because Th lies well above Tg. Therefore, upon undercooling this concentrated PHC solution from T > Tm, homogeneous nucleation would occur at Th within the liquid zone, before vitrification could immobilize the system at Tg. Common examples of PHCs whose actual state diagrams resemble the one in Fig. 12A, and which are known to crystallize readily from concentrated aqueous solution, include xylose (Tm/Tg = 1.51) and glucose (Tm/Tg = 1.42), and to a lesser extent, sucrose (Tm/Tg = 1.43) (refs. 6, 9). The ratios Tm/Th and Tm/Tg reflect the relative distances Tm − Th and Tm − Tg on the mobility transformation map. The secondary influence of the magnitude of Wg' for these PHCs (see Table 2) on the relative mobility within the WLF region is reflected in the greater ease of homogeneous nucleation for glucose than sucrose, since the opposite behavior would be predicted on the basis of the ratio of Tm/Tg alone. Both xylose and glucose exhibit sim-

ple mutarotation in aqueous solution, with their anomeric ratio depending on temperature and concentration (ref. 2). Xylose also exhibits simple mutarotation in the diluent-free melt (ref. 61). For both xylose and glucose, the anomers vitrify compatibly as a single glass. Sucrose, of course, does not exhibit mutarotation and vitrifies as a single glass. In the second case (Fig. 12B), for a PHC with an atypical, lower Tm/Tg ratio < 1.4, homogeneous nucleation would be retarded, because Th falls much closer to Tg, in the more viscous fluid region where transport properties can become a significant limiting factor on nucleation in non-equilibrium systems (ref. 35). Ribose (Tm/Tg = 1.37) is an example of a PHC with a state diagram resembling Fig. 12B, whose nucleation would be so retarded. Ribose exhibits complex mutarotation to six tautomeric and anomeric forms in aqueous solution (ref. 2), which vitrify compatibly as a single aqueous glass. Further study is needed to determine if this existence of multiple conformers contributes to its crystallization inhibition. It is interesting that mannose (Tm/Tg = 1.36), which does not obey the "anomeric rule" (ref. 2) that water favors the species in tautomeric and anomeric equilibria with the largest number of equatorial -OH groups, has a Tm/Tg ratio more like ribose than like glucose, which does obey the rule. In the last case (Fig. 12C), for a PHC with an anomalously low Tm/Tg ratio close to 1.0, homogeneous nucleation would be prevented on a practical timescale, because Th actually lies below Tg. Thus, on undercooling a concentrated solution, vitrification would occur first, thereby immobilizing the system and preventing the possibility of solute nucleation at Th. Fructose (Tm/Tg = 1.06), which is well-known to be almost impossible to crystallize from aqueous solution without preseeding or precipitating with non-solvent, exemplifies the state diagram in Fig. 12C and the nucleation inhibition behavior predicted from it (ref. 9). Like ribose, fructose also exhibits complex mutarotation, with the composition of tautomers and their anomers depending on temperature and concentration (ref. 2). Unlike ribose with its complex mutarotation, or xylose and glucose with their simple mutarotation, the conformers of fructose do not vitrify compatibly as a single glass, as discussed above with regard to the free volume requirements for mobility of fructose conformers. From the standpoint of mechanical relaxations, the compatibility of a solute with the structure of liquid water and the mutual compatibility of a mixture of solutes with water in aqueous glasses are highly cooperative properties, governed by the spatial and orientational requirements for isotropic or anisotropic mobility. From the standpoint of energetics, little is known about cooperative effects which might differentiate between solute-solute or solute-water interactions, but differences in compatibility based on spatial and orientational requirements for labile intermolecular solute-solute and solute-water hydrogen bonds and maintenance of the time-averaged tetrahedral geometry of water are expected to be marginal (ref. 2). Thus, in aqueous solutions and glasses of PHCs, the mutual compatibility of chemically heterogeneous solutes and water is likely to be governed by dynamics and mechanical requirements, rather than energetics. Moreover, the marginal differences in energetics of solute-solute and solute-water interactions are reflected in the limiting partial molar volumes of PHCs, where differences between isomeric sugars are too small to interpret the effect of sugar stereochemistry on hydration (ref. 2) in very dilute solutions. It is suggested that more can be learned about the effect of sugar stereochemistry on the solution behavior of PHCs in the region of the mobility transformation map where dynamics, rather than energetics, dominates (ref. 8).

It should also be noted from the schematic mobility maps in Fig. 12 that the homogeneous nucleation of ice from dilute solutions would not be prohibited during slow cooling, no matter what the Tm/Tg ratio of the PHC solute. Because the Tm/Tg ratio of pure water is about 2.0, its Th lies well above its Tg of about 140°K (ref. 22). The observed Th of pure water is about 233°K (ref. 17), so that its ratio of Tm/Th is about 1.17, which falls at the low end of the reported range of values for essentially all crystallizable substances (refs. 15,71). Thus, at least some of the water in a dilute PHC solution would freeze before it could vitrify, except under extremely fast cooling conditions (ref. 17).

Kinetics of non-equilibrium water sorption

Figure 13 (ref. 13) illustrates the kinetics of water uptake, as a function of environmental RVP at room temperature, in a low-moisture food material representative of other amorphous or partially crystalline substrates. The illustrated sorption behavior reflects both adsorption of water vapor and absorption of condensed liquid water via a diffusion-controlled transport process (i.e. a mechanical relaxation process governed by the mobility of the substrate matrix) (ref. 9). These results of Duckworth were said to "reveal that the time which is required to reach equilibrium conditions needs special attention", and that "equilibration times of at least 14 days might be recommended" (ref. 13). In fact, the results in Fig. 13 demonstrate that times which are orders-of-magnitude greater than 14 days (ref. 11) would be required to approach equilibrium conditions. In such sorption experiments, a low-moisture system may be in an extremely-low mobility, "stationary" solid state so far from equilibrium that it can be easily confused with equilibrium. Figure 13 shows that, even in 25 days, there was no change in water uptake when the environmental relative humidity (RH) was 11%. The essentially immobile solid sample remained far from equilibrium in a low-moisture, negligibly-plasticized "apparent steady state". In sharp contrast, in less than 25 days, there was a dramatic change in water uptake by the same substrate material when the RH was 90%. Under these conditions, the higher-moisture sample was significantly plasticized and exhibited sufficient mobility to allow a more rapid approach toward a still-higher-moisture and not-yet-achieved equilibrium condition. The fundamental trend of increasing sorption rate with increasing environmental RH evidenced by the results in Fig. 13 suggests a mechanistic correlation between increasing mobility and increasing rate of relaxation of the substrate -water system toward its unique final state of equilibrium. This correlation reflects the sequential relationship between increasing water uptake, increasing plasticization, increasing free volume and decreasing local viscosity, which result in decreasing Tg. Viewed in isolation on a practical timescale, the unchanging nature of the low-moisture substrate at low RH would prevent an observer from recognizing this non-equilibrium situation of extremely slow mechanical relaxation.

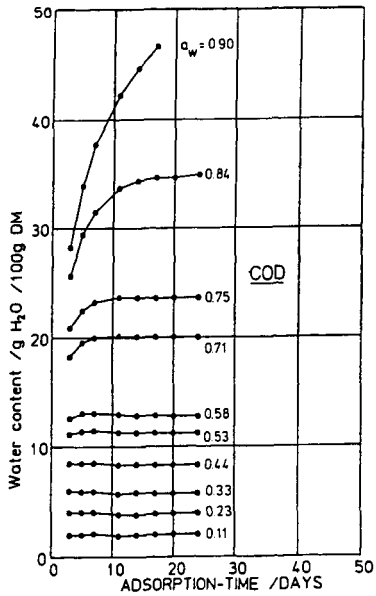

Fig. 13. Water content as a function of adsorption time at different conditions of environmental RVP, illustrating the sorption kinetics of cod at 298°K. [Reproduced, with permission, from ref. 13.]

RVP and Wg′ as functional manifestations of water mobility in small-PHC systems

No discussion of the non-equilibrium behavior of small carbohydrate-water systems could be complete without some mention of "bound water". As reviewed recently elsewhere (e.g. refs. 9,45), "bound" water, in the true sense of the energetics of physical binding, does not exist. Rather, "bound water" (correctly referred to as Wg′ or unfrozen water in the following discussion) and so-called "water activity" (correctly referred to as apparent RVP in the following discussion and next section) are behavioral manifestations of the constrained mobility of water in aqueous PHC glasses and supra-glassy fluids.

As part of an experimental approach to understanding "water dynamics" in intermediate-moisture PHC systems, we have investigated the basis for a relationship between RVP and Wg′ (refs. 4,9). RVP is generally assumed to be an indicator of "free water" content in such intermediate-moisture systems at room temperature (refs. 73,74), while Wg′ is often described as a measure of their "unfreezable" water content (refs. 5-7,19). The study involved a nearly homologous series of sugar syrup solids from commercial high fructose corn, ordinary corn, sucrose, and invert syrups, all of which are commonly used ingredients in "intermediate moisture food" products. RVP was measured for a series of solutions with 67.2 w% solids content after 9 days "equilibration" at 303°K and plotted against Wg′ for maximally-frozen 20 w% solutions of the same solids. The plot (not shown here), with RVP values in the range 0.78-0.98 and Wg′ values in the range 0.5 - 1.0 g unfrozen water/g solute (corresponding Tg′ values in the range 230-254°K), produced a linear correlation coefficient r = -0.71 for the relationship between decreasing content of unfrozen water in the glass at Tg′ and increasing RVP in the corresponding supra-glassy solution some 50-70°K above the Tg′ reference state. The scatter in the data prohibited further insight into the question of water "availability" in such systems. This was not unexpected, since many of the samples represented heterogeneous, polydisperse mixtures of polymeric PHC solutes of unknown average MW, MW distribution, and Tm/Tg ratio. While this study is worth repeating with a homologous series of small monodisperse PHCs, a more definitive and revealing experimental approach to the issue of water "availability" is described in the next section.

Mold spore germination as a mechanical relaxation process

A biological experiment demonstrated that the rates of germination of mold spores in different PHC solutions can be analyzed as a mechanical relaxation process which is governed by the translational mobility of water. In turn, the local effective viscosity of individual supra-glassy PHC solutions at the experimental temperature, which was 50-95°K above their Tg′ reference states, appeared to control the relative mobility of water. Results of the experiment (refs. 4,9) revealed that water mobility can be better understood, explained, and predicted in terms of mobility transformations based on Tg′, Wg′, and the Tm/Tg ratios of PHC solutes of equal MW, rather than the measured RVP of the solutions.

Near room temperature, initial germination of mold spores of Aspergillus parasiticus depends only on the availability of water, not on the presence of nutrients (ref. 72). The experimental protocol, adapted from a microbiological assay used by Lang (ref. 72), compared the inhibitory effects on conidia germination for a series of concentrated solutions of selected PHC and PVP glass-formers. The germination is essentially an all-or-nothing process, with the massive appearance of short hyphae surrounding the previously-bare spores occurring within 1 day at 303°K in pure water or dilute solution (RVP $\cong$ 1.0). The various glass-formers were assayed in pairs, deliberately matched as to the individual parameters of approximately equal RVP (at 303°K), solute concentration, MW, Tg′, and/or Wg′. The relationship between experimental results for number of days required to germinate (as a relaxation time)

and measured solution RVP was scrutinized. These results demonstrated conclusively that the observed rates of germination at 303°K could not be predicted by measured RVPs. However, a conceptual approach based on mobility transformations to describe the kinetics of this mechanical relaxation process in these concentrated, supra-glassy PHC-water systems did facilitate interpretation of the germination data. The illuminating results shown in Table 4 (refs. 4,9) represented a dramatic experimental demonstration of the failure of the "Aw" concept to predict the relative efficacy of PHC additives for antimicrobial stabilization.

TABLE 4. Germination of mold spores of Aspergillus parasiticus in concentrated PHC and PVP solutions.

Design Parameters						Solution		Days Required to Germinate at 303°K
RVP(a) (303°K)	Tg' (°K)	Wg'(b) (w% H_2O)	Tg (°K)	Tm (°K)	Tm/Tg	Conc. (w% H_2O)	Solute Type	
Controls								
1.0						100	None	1
≈1						99	Glucose (α-D)	1
≈1						99	Fructose (ß-D)	1
≈1						99	PVP-40	1
≈1						99	Glycerol	2
0.92	251.5	35	373	---		50	PVP-40	21
0.92	227.5	49.5	302	444.5	1.47	60	α-methyl glucoside(c)	1
0.83	231	49	373	397	1.06	50	Fructose	2
0.83	208	46	180	291	1.62	60	Glycerol	11
0.99	243.5	20	316	402	1.27	60	Maltose	2
0.97	241	36	325	465	1.43	60	Sucrose	4
0.95	250	31	349	406.5	1.16	50	Maltotriose	8
0.93	232	26	303	412.5	1.36	50	Mannose	4
0.95	250	31	349	406.5	1.16	50	Maltotriose	8
0.92	251.5	35	373	---		50	PVP-40	21
0.93	232	26	303	412.5	1.36	50	Mannose	4
0.87	231	49	373	397	1.06	54	Fructose	2
0.92	227.5	49.5	302	444.5	1.47	60	α-methyl glucoside	1
0.87	231	49	373	397	1.06	54	Fructose	2
0.92	227.5	49.5	302	444.5	1.47	60	α-methyl glucoside	1
0.70	231	49	373	397	1.06	30	Fructose	2
0.85	230	29	304	431	1.42	50	Glucose	6
0.83	231	49	373	397	1.06	50	Fructose	2
0.82	230.5	48	293	---		40	1/1 Fructose/Glucose	5
0.98	247	36	339	---		50	PVP-10	11
0.98	231	49	373	397	1.06	60	Fructose	2
0.93	247	36	339	---		40	PVP-10	11
0.95	251.5	35	373	---		60	PVP-40	9
0.99	247	36	339	---		60	PVP-10	11
0.99	243.5	20	316	402	1.27	60	Maltose	2

(a) RVP measured after 7 days "equilibration" at 303°K.
(b) Wg' expressed here in terms of w% water, for ease of comparison with PHC solution concentration.
(c) Commercial material from Staley - Technical grade, used as received.

For the matched pair of fructose and glucose solutions at equal solute concentration, MW, and Tg', fructose produced a much less stable system in which the mold spores germinated much faster, even at slightly lower RVP. Likewise for the matched pairs of fructose vs. glycerol, maltose vs. sucrose, and mannose vs. fructose, the solute with the lower ratio of Tm/Tg allowed faster germination, regardless of RVP values. The Tm/Tg ratio is inversely related to the intrinsic mobility of a solute in its glassy reference state. The temperature difference between the experimental temperature and Tg', and the moisture difference between the water content of the solution and Wg', account for the additional mobility of the experimental system above the reference state. Thus, apparently due to the inherent mobility of a PHC in its glassy reference state and the lower local viscosity and so greater translational mobility in its supra-glassy solution, water availability was greater for fructose (Tm/Tg = 1.06) than mannose (Tm/Tg = 1.36) than glucose (Tm/Tg = 1.42) than glycerol (Tm/Tg = 1.62), and greater for maltose (Tm/Tg = 1.27) than sucrose (Tm/Tg = 1.43). Therefore, greater antimicrobial stabilization was observed for glycerol than glucose than mannose than fructose,

and for sucrose than maltose. The extraordinary mobility and water availability of fructose samples was manifested by the same fast germination time observed for solutions of 40-70 w% fructose and corresponding RVPs of 0.98-0.70. Other noteworthy results in Table 4 involved the matched pairs of PVP-40 vs. methyl glucoside, maltotriose vs. mannose, and PVP-10 vs. fructose, for which Tg' appeared to be the predominant functional determinant. In each case, the solute of higher MW and Tg' manifested lower water availability in its supra-glassy solution (regardless of RVP values), and thus greater stabilization against germination.

Importantly, these experimental germination results were in accord with the unusual behavior often observed for fructose in non-equilibrium, intermediate-moisture food systems (ref.73, 74) and in solutions of similar RVP, in comparison to other more typical monomeric sugars like glucose and mannose, and polyols like glycerol. The microbiological data supported the conclusion (refs. 4,9) that the unusual behavior of fructose is related to its anomalously -low Tm/Tg ratio (calculated based on its second, higher Tg) and resulting low η_g at Tg, and the concomitant high mobility of its glass and supra-glassy solutions. An analysis of the results, in the context of the description of the WLF behavior of polymers with different Tm/Tg ratios discussed with regard to Fig. 4, provided the following key insight. A concentrated fructose solution at 303°K would be about 70°K above its Tg' reference state. Such a supra-glassy fructose solution would exhibit anomalously low local viscosity at this temperature due to two factors related to the low Tm/Tg ratio of fructose. The magnitude of the WLF rubbery range is smaller for a lower Tm/Tg ratio, so that the fructose solution would exist as a liquid well ABOVE its WLF rubbery range. The local viscosity in the glassy reference state is lower for a lower Tm/Tg ratio, so that the viscosity of the fructose solution would be lower than could be accounted for by the temperature difference alone. In contrast, at the same experimental temperature and almost the same temperature difference above Tg', supra-glassy solutions of glucose (Tm/Tg = 1.42) or mannose (Tm/Tg = 1.36), or even glycerol (Tm/Tg = 1.62), at a still greater temperature difference (95°K) above its Tg', would exist as higher-viscosity fluids WITHIN their WLF rubbery range. Thus, like the lower viscosity fructose-water reference glass at Tg, the fructose solution well above Tg would be a much more mobile system than the corresponding glucose, mannose, and glycerol solutions. Consequently, a mechanical relaxation process dependent on translational diffusion, as exemplified by the germination of mold spores, was able to occur more quickly in a fructose solution than in solutions of glucose, mannose, or glycerol of equal or higher RVP. It is especially noteworthy that the same apparent correlations among low local effective viscosity, fast translational diffusion, high translational mobility, short translational relaxation time, and low Tm/Tg ratio, are suggested here by the results for mold spore germination rates in small PHC-water systems at 50 - 95°K above Tg', as suggested earlier from the analysis of translational friction coefficients in Fig. 11 for synthetic high polymers at 100°K above Tg.

Finally, the 1:1 fructose:glucose mixture in Table 4 deserves special mention, because of its importance in many technological applications, including intermediate-moisture foods, and because of its significant contribution to our theoretical interpretation of the non -equilibrium behavior of PHC-water systems. The germination time for mold spores in a concentrated solution of this mixture was much more like that of a solution of glucose alone than fructose alone, which indicates that the mechanical relaxation behavior of the solution mixture is quite similar to that of a glucose solution with respect to TRANSLATIONAL mobility. A 20 w% solution of the mixture showed a Tg' intermediate between the values for fructose and glucose, but a Wg' almost identical to the value for fructose alone. The glass curves of Fig. 5 reveal that 1) the predominant conformer of fructose in its mechanically and spatially homogeneous vitrified aqueous solutions is the one responsible for the higher Tg value of dry fructose alone at 373°K, and 2) the anomalously large value of Wg' for aqueous solutions of fructose alone results from the free volume requirement for rotational mobility of this "anisotropic" fructose conformer. This important conclusion concerning the identity of the predominant fructose conformer in aqueous fructose glasses is demanded by the recognition, gained from the vast literature for plasticized synthetic polymers (refs. 20,37), that the glass curve always exhibits a smooth monotonic decrease in Tg with increase in plasticizer content expressed as a weight fraction (free volume in the plasticized blend is additive or cumulative, depending on the disparity in MW, on a weight fraction basis), with no local maxima unless stoichiometric complexes arise in particular composition ranges. Thus, the mechanical behavior of the solution of the 1:1 mixture of glucose with fructose is dominated by the free volume requirements of the "anisotropic" fructose conformer, with respect to ROTATIONAL mobility. As mentioned earlier, the mechanically homogeneous dry glass obtained by melting a 1:1 mixture of ß-D-fructose and α-D-glucose exhibited only one Tg at 293°K, exactly intermediate between the Tg of dry glucose alone at 304°K and the Tg of the second conformer of dry fructose at 284°K. It appears that the predominant fructose conformer in the mixed dry glass is the second, glucose-like or "isotropic" conformer, with the lower of the two Tg values of fructose. In summary, the germination time for the solution mixture was determined by its constrained translational mobility. The constraint was much greater than for a solution of fructose alone and somewhat less than for a solution of glucose alone. This constrained translational mobility in the supra-glassy fluid was related to the single dry Tg of the mixture, which was much closer to that of glucose, with its higher value of Tm/Tg, than to that of the anomalous conformer of fructose, with its very low value of Tm/Tg. We conclude that the apparent RVP (so-called Aw) of a concentrated PHC solution does not control water availability, but is simply another diagnostic manifestation, like the times required for spore germination, of the non-equilibrium translational relaxation behavior of the solution. It is suggested that the anomalous fructose conformer is the predominant species in aqueous fructose glasses and in aqueous glasses of the 1:1 mixture of fructose and glucose, that the anomalous fructose conformer is mechanically incompatible with the glucose-like fructose conformer in the dry melt of fructose alone, and that the glucose-like fructose conformer is the predominant species in the single dry glass of the 1:1 mixture. We hope that this speculative discussion, which should provide pregnant clues to one versed in the stereochemistry of small PHCs, may provoke appropriate experimentation

with molecular modelling, NMR, and dielectric relaxation techniques to explore the effects of concentration, temperature, and pressure on the nature and kinetics of conformational changes during melting and vitrification of dry PHC systems and their aqueous solutions.

Further comments on the fructose vs. glucose paradox

In the field of food technology, comparisons of the technological properties of the three most readily-available sugars, fructose, glucose, and sucrose, are important and topical. Especially for applications involving the "moisture management" of intermediate-moisture foods, the choice between fructose and glucose to depress RVP and thus increase shelf life is often controversial, confusing, and contradictory (ref. 9). The situation can be summarized by the following paradoxical "truths" (refs. 73,74). In foods with limited total moisture, formulation on an equal weight basis with fructose rather than glucose typically results in a lower value of apparent RVP and greater storage stability, because the much greater solubility of fructose results in a greater effective concentration of fructose than glucose. However, if a product is formulated with glucose to achieve a certain RVP value which has been empirically demonstrated to provide stability with respect to a particular test microorganism, then reformulation with fructose to the same RVP often produces a less stable product. This is so, because less fructose than glucose is required to achieve the same RVP, while, as illustrated by the mold spore germination results in Table 4, at the same RVP, fructose solutions are less stable than glucose solutions (ref. 9).

Since the colligative depression of the equilibrium water activity is the same for infinitely dilute solutions of fructose and glucose, the traditional approach to the fructose vs. glucose paradox has been to question why the observed RVP of a fructose solution of finite or high concentration is significantly lower than that of a glucose solution of equivalent concentration. A further comparison of the glass curves in Fig. 5 leads us to conclude that a concentrated fructose solution is anomalous, because its RVP is not depressed ENOUGH relative to that of glucose. In other words, we need to ask the opposite question - why is the RVP for a fructose solution so HIGH, for such a small vector above its glass curve? For the technologically practical case of a 50 w% solution at room temperature, the temperature differential (ΔT) or the water differential (ΔW) above the reference glass curve in Fig. 5 is much smaller for fructose than for glucose. One would therefore expect the translational mobility of water in the fructose solution so close to its glass curve to be more restricted (i.e. lower RVP) than it appears to be. We suggest that the explanation lies in the anomalously-large free volume requirement for rotational mobility in the supra-glassy fluid (as reflected in the very low value of Tm/Tg ratio), which results in anomalously-low local viscosity. Thus, translational diffusion in the supra-glassy fructose solution is very rapid (relative to that in the solution of glucose, with its much higher Tm/Tg ratio), and the depression of its non-equilibrium RVP is less than expected.

Starch gelatinization as a mechanical relaxation process affected by the mobility of aqueous sugar solutions

Another experimental approach to study the relative translational mobility of aqueous sugar solutions involves the use of starch, a high-polymeric PHC, as a reporter molecule, instead of water. Gelatinization of native, partially crystalline, granular starch is a mechanical relaxation process with non-Arhennius kinetics which depend on the mobility of the added plasticizer. Gelatinization of starch in water, as a consequence of heat-moisture treatment, is a non-equilibrium melting process (ref. 26), which becomes cooperative and occurs at a significant rate at a characteristic temperature (Tgelat) corresponding to the instantaneous Tg (i.e. Tgelat = Tg) of the water-plasticized amorphous regions of the amylopectin (refs. 47,57,58). Gelatinization in concentrated aqueous solutions of common sugars begins at a higher Tgelat than in water alone, a retardation effect suggested to result from "antiplasticization" (as defined for synthetic polymers (ref. 37)) by sugar-water co-solvents, relative to the extent of plasticization by water alone. Sugar-water, of higher average MW than water, results in a smaller depression of starch Tg than does water (refs. 47,57). In fact, isothermal treatment of starch in sugar-water, at a temperature which would result in non-equilibrium melting of amylopectin in water alone, results in antiplasticization by annealing and crystallite perfection instead (ref. 57). Investigation of the non-equilibrium relaxation behavior of different supra-glassy sugar-water solutions, in the context of the effect of their translational mobility on the diffusion-controlled Tgelat of partially crystalline starch, is greatly enhanced by the simultaneous investigation of their rotational mobility, as measured by dielectric relaxation.

The dielectric relaxation time, τ, for a small PHC in aqueous solution is directly related to the rotational diffusion time. Maximum absorbance of electromagnetic radiation by pure water at room temperature occurs at a frequency of $\backsimeq$ 17 GHz in a microwave dielectric dispersion experiment. Microwave absorption maxima at lower frequencies result when free volume becomes limiting and relaxations occur at lower frequencies due to hindered rotation. For comparison, the commercial frequency used for domestic microwave ovens is 2.45 GHz. In the case of a dilute solution, when free volume is not limiting, the dielectric relaxation time is determined mainly by the intrinsic hydrodynamic volume of the solute (refs. 66-68). For each small PHC solute in water at a given temperature, there is a limiting concentration below which the mobility shows simple dependence on the average molar volume and above which the free volume limitation would begin to contribute to hindered rotation and increased local viscosity (which is equivalent to macroscopic solution viscosity for MW below the entanglement limit). At 293°K, this limiting concentration has been shown to be $\backsimeq$ 33 w% for sucrose and $\backsimeq$ 38 w% for glucose (ref. 22). In other words, the hindered mobility characteristic of WLF behavior in the "rubbery" domain would be observed when $\Delta T \backsimeq 52°K$ and $\Delta W \backsimeq 31$ w% above the Tg'-Wg' reference state for a sucrose solution and when $\Delta T \backsimeq 63°K$ and $\Delta W \backsimeq 33$ w% above the Tg'-Wg' reference state for a glucose solution.

Suggett and Clark (ref. 68) have assessed the rotational diffusion behavior of concentrated aqueous solutions (24.0-33.5 w% solute) of a series of small sugars, including the pentoses ribose and xylose, the hexoses glucose and mannose, and the disaccharides sucrose and maltose. They determined dielectric relaxation times from microwave dispersion measurements made over a frequency range from 100 KHz to 35 GHz at 278°K, where these supra-glassy sugar solutions would be expected to exhibit hindered rotation and the WLF behavior mentioned above. We have assessed the effect of the same sugars on starch gelatinization, from DSC measurements of Tgelat for native granular wheat starch suspensions in 50 w% aqueous sugar solutions (ref. 57). We can estimate the relative effects of the different sugar solutions on translational diffusion in the sugar-water-starch suspension from these measurements of Tgelat, which reflect the relative deficit in depression of Tg of the amylopectin component of starch by sugar-water compared to water alone (refs. 47,57,58). As revealed by the graph of Tgelat vs. dielectric relaxation time (picoseconds) in Fig. 14, the effects of these sugars on starch gelatinization are highly linearly correlated (r = 0.97) with their rotational diffusion times in solution, as measured by dielectric relaxation. It is especially interesting to note that the surprising behavior of glucose and its dimer, maltose, which show very similar rotational diffusion times, is reflected in exactly the same way by their very similar effect on Tgelat for the mechanical relaxation process reported by starch.

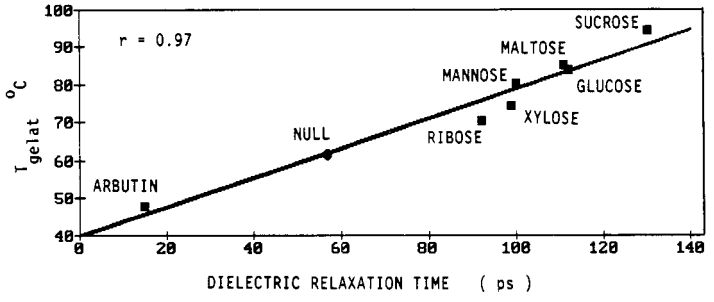

Fig. 14. The variation of the gelatinization temperature of native wheat starch suspended in 50 w% aqueous sugar solutions with the corresponding dielectric relaxation time measured at 278°K for concentrated aqueous solutions of the same sugars.

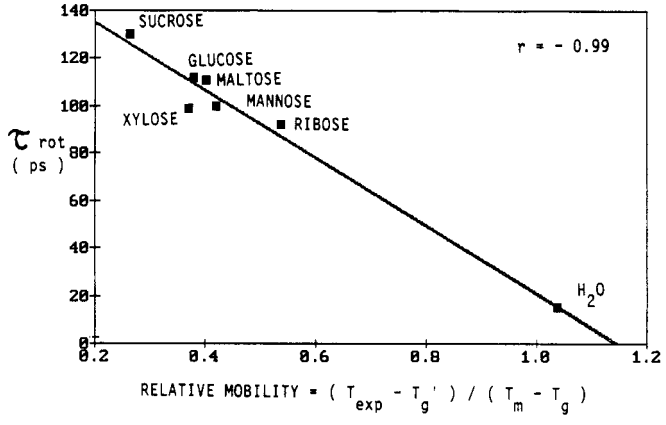

Fig. 15. The variation of rotational diffusion time measured at 278°K for concentrated aqueous sugar solutions with the corresponding relative mobility parameter of aqueous solutions of the same sugars, calculated from the ratio of (Texp - Tg')/(Tm - Tg) for each sugar.

We suggest that the underlying explanation for this correlation is revealed by the graph in Fig. 15, which shows the fundamental relationship between the measured rotational diffusion times from the dielectric relaxation experiment (ref. 68) and the calculated relative mobilities of the supra-glassy sugar-water solutions. A relaxation transformation map was constructed for each sugar solution, and relative mobility was estimated from the relative distance between the experimental conditions and the reference glass curve, normalized with respect to the inherent mobility of the PHC. As stated previously, the inherent mobility of a PHC is related to the distance (in units of temperature) required by its dry glass to achieve the mobility of an Arrhenius liquid. Thus, the relative mobility scale shown in Fig. 15, calculated for each sugar from the ratio of $(T - Tg')/(Tm - Tg)$, is defined in terms of the temperature difference between the experimental temperature (278°K) and Tg' of the freeze-concentrated glass as the reference state, compared to the magnitude of the temperature difference in the WLF domain between Tm and Tg of the dry solute as a measure of inherent mobility. Both dielectric relaxation times and translational diffusion coefficients of a broad range of glass-forming systems, including polyvinyl acetate and glucose, have been shown experimentally to follow the WLF eqn. near Tg (refs. 75,77). As noted earlier, the factor $(Tm - Tg)$ was chosen, in this case as a preferred alternative to the Tm/Tg ratio, for the comparison of mobilities, at $T >> Tg$, of different small PHCs with different values of dry Tg (see Table 1). Fig. 15 illustrates the excellent linear correlation (r = 0.99) between the mobility, expressed in terms of WLF behavior, and the dielectric relaxation behavior of the aqueous sugar solutions in their non-equilibrium, supra-glassy states. As expected, in the absence of anomalous anisotropic requirements of free volume for mobility, both translational and rotational mobility depend correlatively on free volume, but translational motion becomes limiting at a higher temperature and determines Tg. It should be noted that the calculated translational mobility for xylose is significantly lower than expected, based on its rotational relaxation time. The high value of Tm/Tg for xylose accounts for the low calculated mobility, which has been confirmed experimentally by demonstrating the anomalous ability of xylose to retard the recrystallization of starch (ref. 57).

CONCLUSION

The stated objective of the symposium on the physical chemistry of small carbohydrates, at which this paper was presented, was to bring together scientists from applied and basic research areas, and from industrial and academic labs, for an unusual exchange of ideas. In this paper, we have emphasized the importance of the non-equilibrium behavior of small carbohydrate-water systems of finite concentration, which are governed by dynamics rather than energetics, because of their strategic role in situations of biological stress and for technological applications where conditions of temperature, concentration, and pressure are usually far from equilibrium and practical timescales are utterly inadequate for the approach to equilibrium. We have described a new theoretical and experimental framework (developed from structure/property principles established for synthetic high polymers) for the treatment of such systems, which focuses on their kinetic description, facilitates time-temperature-concentration-pressure superpositions through underlying mobility transformations, and establishes reference conditions of temperature and concentration characteristic of each solute. We have illustrated the perspective afforded by using this conceptual framework to approach questions concerning the dynamically-constrained behavior of small carbohydrates which exist in glassy and "rubbery" states and are subject to plasticization by water. Finally, we have proposed that small carbohydrate-water systems are uniquely well-suited for the investigation of non-equilibrium behavior: the definition of conditions for its empirical demonstration, the examination of materials properties that allow its description and control, the identification of appropriate experimental approaches, and the exploration of theoretical interpretations.

Acknowledgements

We thank Nabisco Brands for permission to publish this paper, and our friend and mentor, Prof. Felix Franks, for many years of scientific stimulation and professional encouragement.

REFERENCES

1. F. Franks, in Polysaccharides in Food (eds. J.M.V. Blanshard and J.R. Mitchell), p. 33, Butterworths, London (1979).
2. F. Franks, Pure & Appl. Chem. 59, 1189-1202 (1987).
3. H. Levine and L. Slade, Carbohydr. Polym. 6, 213-244 (1986).
4. L. Slade and H. Levine, in Food Structure - Its Creation and Evaluation (eds. J.R. Mitchell and J.M.V. Blanshard), chap. 8, Butterworths, London (1987).
5. H. Levine and L. Slade, in Food Structure - Its Creation and Evaluation (eds. J.R. Mitchell and J.M.V. Blanshard), chap. 9, Butterworths, London (1987).
6. H. Levine and L. Slade, in Water and Food Quality (ed. T.M. Hardman), in press, Elsevier Applied Science, London (1988).
7. H. Levine and L. Slade, Cryo-Letters 9, 21-63 (1988).
8. H. Levine and L. Slade, J. Chem. Soc., Faraday Trans. 1, in press (1988).
9. H. Levine and L. Slade, in Water Science Reviews (ed. F. Franks), Vol. 3, p. 79, Cambridge University Press, Cambridge (1987).
10. H. Weisser, in Properties of Water in Foods (eds. D. Simatos and J.L. Multon), p. 95, Martinus Nijhoff, Dordrecht (1985).
11. H. Bizot, A. Buleon, N. Mouhous-Riou and J.L. Multon, in Properties of Water in Foods (eds. D. Simatos and J.L. Multon), p. 83, Martinus Nijhoff, Dordrecht (1985).
12. C. van den Berg, in Concentration and Drying of Foods (ed. D. MacCarthy), p. 11, Elsevier Applied Science, London (1986).
13. W. Wolf, W.E.L. Spiess and G. Jung, in Properties of Water in Foods (eds. D. Simatos and J.L. Multon), p. 661, Martinus Nijhoff, Dordrecht (1985).
14. B. Wunderlich, Macromolecular Physics, Vol. 1 - Crystal Structure, Morphology, Defects, Academic Press, New York (1973).
15. B. Wunderlich, Macromolecular Physics, Vol. 2 - Crystal Nucleation, Growth, Annealing, Academic Press, New York (1976).
16. B. Wunderlich, Macromolecular Physics, Vol. 3 - Crystal Melting, Academic Press, New York (1980).
17. F. Franks, in Water: A Comprehensive Treatise (ed. F. Franks), Vol. 7, p. 215, Plenum Press, New York (1982).
18. F. Franks, Biophysics and Biochemistry at Low Temperatures, Cambridge University Press, Cambridge (1985).
19. F. Franks, in Properties of Water in Foods (eds. D. Simatos and J.L. Multon), pp. 1,497, Martinus Nijhoff, Dordrecht (1985).
20. J.D. Ferry, Viscoelastic Properties of Polymers, 3rd edn., John Wiley & Sons, New York (1980).
21. M.L. Williams, R.F. Landel and J.D. Ferry, J. Amer. Chem. Soc. 77, 3701-3706 (1955).
22. T. Soesanto and M.C. Williams, J. Phys. Chem. 85, 3338-3341 (1981).
23. J.A. Brydson, in Polymer Science (ed. A.D. Jenkins), p. 194, North Holland, Amsterdam (1972).
24. G.E. Johnson, H.E. Bair, S. Matsuoka, E.W. Anderson, and J.E. Scott, in Water in Polymers (ed. S.P. Rowland), ACS Symp. Ser. 127, p. 451, American Chemical Society, Washington, D.C. (1980).
25. R.N. Haward, The Physics of Glassy Polymers, Applied Science Publ., London (1973).
26. B. Wunderlich, in Thermal Characterization of Polymeric Materials (ed. E.A. Turi), p. 91, Academic Press, Orlando (1981).

27. F. Franks, in Effects of Low Temperatures on Biological Membranes (eds. G.J. Morris and A. Clarke), p. 3, Academic Press, London (1981).
28. U. Bengtzelius and A. Sjolander, in Conference on Dynamic Aspects of Structural Change in Liquids and Glasses, abs. 16, New York Acad. Sci., New York, Dec. 1-3 (1986).
29. C.R. Cantor and P.R. Schimmel, Biophysical Chemistry - Part II: Techniques for the Study of Biological Structure and Function, W.H. Freeman & Co., San Francisco (1980).
30. K.E. Van Holde, Physical Biochemistry, Prentice-Hall, Englewood Cliffs (1971).
31. A. Eisenberg, in Physical Properties of Polymers (eds. J.E. Mark, A. Eisenberg, W.W. Graessley, L. Mandelkern, and J.L. Koenig), p. 55, American Chemical Society, Washington, D.C. (1984).
32. H.E. Bair, Polym. Prepr. 26, 10 (1985).
33. V.N. Morozov and S.G. Gevorkian, Biopolymers 24, 1785-1799 (1985).
34. D.R. Buchanan and J.P. Walters, Textile Res. J. 47, 398-406 (1977).
35. I.H. Leubner, J. Phys. Chem. 91, 6069-6073 (1987).
36. H.E. Bair, in Thermal Characterization of Polymeric Materials (ed. E.A. Turi), p. 845, Academic Press, Orlando (1981).
37. J.K. Sears and J. R. Darby, The Technology of Plasticizers, Wiley-Interscience, New York (1982).
38. A.P. MacKenzie, Phil. Trans. R. Soc. Lond. B. 278, 167-189 (1977).
39. A.P. MacKenzie and D.H. Rasmussen, in Water Structure at the Water-Polymer Interface (ed. H.H.G. Jellinek), p. 146, Plenum Press, New York (1972).
40. F. Franks, J. Microsc. 141, 243-249 (1986).
41. H. Kanno, J. Phys. Chem. 91, 1967-1971 (1987).
42. A.P. MacKenzie, in Freeze Drying and Advanced Food Technology (eds. S.A. Goldlith, L. Rey, and W.W. Rothmayr), p. 277, Academic Press, New York (1975).
43. F.W. Billmeyer, Textbook of Polymer Science, 3rd edn., Wiley-Interscience, New York (1984).
44. W.W. Graessley, in Physical Properties of Polymers (eds. J.E. Mark, A. Eisenberg, W.W. Graessley, L. Mandelkern, and J.L. Koenig), p. 97, American Chemical Society, Washington, D.C. (1984).
45. L. Slade, H. Levine and J.W. Finley, in Influence of Processing on Food Proteins (eds. D. Phillips and J.W. Finley), Marcel Dekker, New York, 9-124 (1988).
46. S. Quinquenet, C. Grabielle-Madelmont, M. Ollivon and M. Serpelloni, J. Chem. Soc., Faraday Trans. 1, in press (1988).
47. L. Slade, in American Association of Cereal Chemists 69th Annual Meeting, Minneapolis, MN, abs. 112, (1984).
48. K.J. Zeleznak and R.C. Hoseney, Cereal Chem. 64, 121-124 (1987).
49. J.M.V. Blanshard, in Food Structure - Its Creation and Evaluation (eds. J.R. Mitchell and J.M.V. Blanshard), Butterworths, London, 313-330 (1987).
50. L. Slade and H. Levine, in Advances in Meat Research, Vol. 4 (eds. A.M. Pearson, T.R. Dutson and A.J. Bailey), p. 251, AVI, Westport (1987).
51. H. Batzer and U.T. Kreibich, Polym. Bull. 5, 585-590 (1981).
52. S.R. Kakivaya and C.A.J. Hoeve, Proc. Nat. Acad. Sci. USA 72, 3505-3507 (1975).
53. R.C. Hoseney, K. Zeleznak and C.S. Lai, Cereal Chem. 63, 285-286 (1986).
54. W.J. Sichina, Amer. Lab. 20(1), 42-52 (1988).
55. G.E. Downton, J.L. Flores-Luna and C.J. King, Ind. Eng. Chem. Fundam. 21, 447-451 (1982).
56. D.C. Bonner and J.M. Prausnitz, J. Polym. Sci.: Polym. Phys. Ed. 12, 51-73 (1974).
57. L. Slade and H. Levine, in Recent Developments in Industrial Polysaccharides (eds. S.S. Stivala, V. Crescenzi and I.C.M. Dea), p. 387, Gordon & Breach Science, New York (1987).
58. L. Slade and H. Levine, Carbohydr. Polym. 8, 183-208 (1988).
59. C. van den Berg, Doctoral Thesis, Agricultural University, Wageningen (1981).
60. F. Franks, personal communication (1987).
61. F. Shafizadeh, G.D. McGinnis, R.A. Susott and H.W. Tatton, J. Org. Chem. 36, 2813-2818 (1971).
62. H. Kanno, K. Shimada and T. Katoh, in 8th International Symposium on Solute-Solute-Solvent Interactions (eds. J. Barthel and G. Schmeer), p. 66, University of Regensburg, Federal Republic of Germany (1987).
63. R. Vassoille, A. El Hachadi and G. Vigier, Cryo-Lett. 7, 305-310 (1986).
64. D.R. MacFarlane, Cryo-Lett. 6, 313-318 (1985).
65. P. Boutron and A. Kaufmann, Cryobiology 16, 557-568 (1979).
66. M.J. Tait, A. Suggett, F. Franks, S. Ablett and P.A. Quickenden, J. Solution Chem. 1, 131-151 (1972).
67. F. Franks, D.S. Reid and A. Suggett, J. Solution Chem. 2, 99-118 (1973).
68. A. Suggett and A.H. Clark, J. Solution Chem. 5, 1-15 (1976).
69. A. Suggett, S. Ablett and P.J. Lillford, J. Solution Chem. 5, 17-31 (1976).
70. A. Suggett, J. Solution Chem. 5, 33-46 (1976).
71. A.G. Walton, in Nucleation (ed. A.C. Zettlemoyer), p. 225, Marcel Dekker, New York (1969).
72. K.W. Lang, Doctoral Thesis, University of Illinois (1981).
73. M. Loncin, in Freeze Drying and Advanced Food Technology (eds. S.A. Goldlith, L. Rey, and W.W. Rothmayr), p. 599, Academic Press, New York (1975).
74. J. Chirife, G. Favetto and C. Fontan, Lebensm.-Wiss. u.-Technol. 15, 159-160 (1982).
75. S. Matsuoka, G. Williams, G.E. Johnson, E.W. Anderson and T. Furukawa, Macromolecules 18, 2652-2663 (1985).
76. S.E.B. Petrie, in Polymeric Materials: Relationships Between Structure and Mechanical Behavior (eds. E. Baer and S.V. Radcliffe), p. 55, Amer. Soc. Metals, Ohio (1975).
77. W.J. Huang, T.S. Frick, M.R. Landry, J.A. Lee, T.P. Lodge and M. Tirrell, AIChE Journal 33, 573-582 (1987).
78. D.R. MacFarlane, R.K. Kadiyala and C.A. Angell, J. Phys. Chem. 87, 1094-1095 (1983).